Geospatial modelling of large wood supply to rivers: a state-of-the-art model comparison in Swiss mountain river catchments

Nicolas Steeb[1,*], Virginia Ruiz-Villanueva[2,3], Alexandre Badoux[1], Christian Rickli[1], Andrea Mini[3], Markus Stoffel[2,4,5], Dieter Rickenmann[1]

[1]Swiss Federal Research Institute WSL, Zürcherstrasse 111, CH-8903 Birmensdorf, Switzerland

[2]C-CIA-Climate Change Impacts and Risks in the Anthropocene, Institute for Environmental Sciences (ISE), University of Geneva, CH-1205 Geneva, Switzerland

[3]Institute of Earth Surface Dynamics (IDYST), University of Lausanne, UNIL Mouline, CH-1015 Lausanne, Switzerland

[4]Dendrolab.ch, Department of Earth Sciences, University of Geneva, Geneva, Switzerland.

[5]Department F.-A. Forel for Environmental and Aquatic Sciences, University of Geneva, Geneva, Switzerland

*Corresponding author: Nicolas Steeb, Email: nicolas.steeb@wsl.ch

ABSTRACT

Different models have been used in science and practice to identify instream large wood (LW) sources and to estimate LW supply to rivers. This contribution reviews the existing models proposed in the last 35 years and compares two of the most recent GIS-based models by applying them to 40 catchments in Switzerland. Both models, which we call here empirical GIS approach (EGA) and Fuzzy-Logic GIS approach (FGA), consider landslides, debris flows, bank erosion, and mobilization of instream wood as recruitment processes and compute volumetric estimates of LW supply based on three different scenarios of process frequency and magnitude. Despite being developed following similar concepts and fed with similar input data, the results from the two models differ markedly. In general, estimated supply wood volumes were larger in each of the scenarios when computed with the FGA and lower with the EGA models. Landslides were the dominant process identified by the EGA, whereas bank erosion was the predominant process according to the FGA model. These differences are discussed, and results are compared to available observations coming from a unique database. Regardless of the limitations of these models, they are useful tools for hazard assessment, the design of infrastructure, and other management strategies.

KEYWORDS: large wood, GIS, modelling, landslide, bank erosion, debris flow, natural hazards

1 INTRODUCTION

The influence of wood in watercourses is manifold. On the one hand, there are various ecological benefits of large wood (LW), as it provides habitats and a food source for many organic organisms, thus promoting rich biodiversity (Harmon et al., 2004; Steel et al., 2003; Wondzell and Bisson, 2003). LW also affects stream hydraulics by altering the channel morphology and sediment control (Montgomery and Piégay, 2003; Wohl and Scott, 2016). On the other hand, large quantities of LW may be mobilized during infrequent, high-magnitude floods and may induce potential hazards for human settlements and infrastructure (Lucía et al., 2015c; Lucía et al., 2018; Rickli et al., 2018; Ruiz-Villanueva et al., 2013; Steeb et al., 2017b). Consequently, river managers are challenged to maintain a good ecological status of rivers while minimizing potential hazards.

From a flood protection perspective, the main problem regarding LW in streams is wood accumulation at bridges, and weirs, which reduces or even clogs the entire river cross section and leads to backwater rise and consequent inundation (Comiti et al., 2016; Lassettre and Kondolf, 2012; Piégay et al., 1999; Rickenmann et al., 2016). The associated damage potential of LW may depend, among other variables, on the volume of transported LW (Mazzorana et al., 2018). Large wood transport is governed by the flow conditions, river morphology (Ruiz-Villanueva et al., 2020), the size and shape of individual wood pieces (i.e., large logs or rootwads are more prone to clogging; Bezzola et al., 2002), the mode wood is being transported (i.e., if logs are transported congested or not; Braudrick et al., 1997; Ruiz-Villanueva et al., 2019) and the availability or supply of wood. Wood supply occurs by numerous geomorphic processes including bank erosion, channel migration, mass wasting (e.g., landslides, debris flows) and natural tree mortality and fall (Benda and Sias, 2003). These processes can be highly variable, both on temporal and spatial scales (Gasser et al., 2019).

Despite numerous existing approaches and efforts (see following section), the quantitative estimation of LW supply volume and the definition of contributing source areas based on different recruitment processes remain very challenging. The estimation of exported wood involves many

uncertainties that are difficult to quantify, because LW transport happens at the end of a long process cascade, usually starting with precipitation as a trigger, followed by a flood formation and the occurrence of recruitment processes as wood suppliers, and the increased discharge as a transport medium. In addition, any type of model developed to estimate and quantify wood supply should be validated with field observations, data that is very scarce (Comiti et al., 2016; Nakamura et al.., 2017; Wohl et al., 2019; Gurnell & Bertoldi, 2020).

This work reviews the state-of-the-art in wood supply modelling and presents a comparison of two recent GIS-based approaches that were developed in the context of an applied research project funded by the Swiss Federal Office for the Environment. First, the literature review provides an updated compilation of published approaches to model recruitment processes to quantify LW supply, classifying the approaches by model type and summarizing their main characteristics, such as processes considered, and their temporal and spatial scales. We then focus on two GIS-based models that were developed based on a similar general concept, used similar input data, and were applied to the same study sites. The models were validated with a unique observation dataset of supplied wood during single events in a large number of catchments in Switzerland (Steeb, 2018; Steeb et al., 2019a). Despite their similarities, the models differ in some respects and result in somewhat different outcomes. These differences are used to stress the limitations and strengths of the two models, to compare them with other recent approaches included in the literature review and to discuss uncertainties and challenges related to the modelling of LW supply. In addition, we also consider implications for flood hazard assessment and river management.

2 LARGE WOOD SUPPLY MODELS: A REVIEW

Over the last decades, different approaches have been developed to quantify LW supply at both, reach and catchment scales. Gregory et al. (2003) provided a summary of the first attempts to simulate wood supply, i.e., mostly mathematical models developed from conceptual descriptions of selected wood recruitment processes. Later, Gasser et al. (2019) reviewed recent approaches and evaluated whether the stabilizing effect of vegetation on total LW supply was considered or not. In this work, we compile and expand these previous overviews to provide an updated review of published approaches to model recruitment processes and to quantify LW supply (Table 1; numbering therein used for reference in this section). We classify the approaches by model category (i.e., empirical, deterministic, stochastic, or GIS-based) and summarize their main characteristics (i.e., processes considered, spatial and temporal scales, inputs and outputs, and whether they were validated with field observations or not). The evolution of these models illustrates and contributes to the scientific understanding of the complex processes involved in wood supply to rivers. Some of the earliest approaches, e.g., [1], [21], [22], were designed to simulate long-term delivery of wood to river reaches from adjacent riparian forest by tree mortality, windthrow or bank erosion. Subsequent models attempted to describe these input processes over larger portions of river networks [3], [4], [6], [23], [24], but maintained a long-term perspective. Few studies included other processes, such as channel avulsion [4], [22]. These earlier models were developed in the US, most of them in the Pacific Northwest and a few in the Southeast [4] or the Rocky Mountains [23]. Later, researchers started to apply and develop models elsewhere, e.g., in New Zealand [24].

Martin and Benda (2001) and Benda and Sias (2003) [16] were pioneers in considering mass movements (i.e., landslides and debris flows) as wood recruitment processes, and they established the first conceptual framework for LW budgeting. This approach has been further applied in US mountain rivers [8], [20] before it has been adapted to shorter timescales for mountain rivers in Italy and Switzerland [14], [29]. Focusing on shorter time windows and on episodic disturbances (e.g., floods) aggregated at the catchment scale, researchers proposed empirical equations based

114 on field observations of exported wood and catchment characteristics [28], [29]. As most of the
115 data used to derive such empirical formulas originated from steep headwater streams and
116 mountain rivers in Switzerland, Austria, and Japan, application to larger catchments is associated
117 with considerable uncertainty.

118 The rapid proliferation of remote sensing and the advances in computing sciences and
119 geographic information systems (GIS; Bishop and Giardino, 2022) resulted in the development
120 of another group of models (i.e., geospatial models). These GIS-based models allow a spatially
121 explicit assessment of different LW recruitment processes, the identification of source areas and
122 the estimation of LW volumes, expanding the analysis to larger areas, covering multiple (sub-
123)catchments. Rimböck (2001) [5] developed a GIS-based model to identify potential recruitment
124 areas of LW in mountain streams, resulting from bank erosion, landslides and windthrow. In this
125 approach, he used wood volume reduction factors to distinguish between the potential LW volume
126 (i.e., maximum volume that could potentially be supplied) and the estimated wood volume
127 exported or supplied during exceptional floods. Mazzorana et al. (2009) [10] developed a
128 procedure to determine the relative propensity of mountain streams in Bolzano Province (Italy)
129 to supply wood due to floods, debris flows in tributaries, bank erosion and shallow landslides,
130 based on empirical indicators. Kasprak et al. (2012) [18] used light detection and ranging
131 (LiDAR) data to estimate tree height and recruitable tree abundance throughout a watershed in
132 US Coastal Maine, and to determine the likelihood for the stream to recruit channel-spanning
133 trees at the reach scale and assess whether mass wasting or channel migration was a dominant
134 supply mechanism. Ruiz-Villanueva et al. (2014c) [12] estimated potential LW volumes recruited
135 from landslides, bank erosion and fluvial transport during floods in the Central Mountain Range
136 in Spain. The authors applied a GIS model including multi-criteria and multi-objective
137 assessments using fuzzy logic principles together with reduction factors for predefined scenarios.
138 The method included the analysis of the hillslope-channel network connectivity and the resistance
139 of the vegetation to be eroded. This approach was recently adapted and applied to mountain
140 catchments in Switzerland, considering debris flows as supply processes as well [13], and it has

been further used in the present study. Also applied in Swiss mountain catchments, Steeb et al. (2017a, 2019b) [11] proposed a GIS approach to model source areas of LW and to estimate potential supply and exported wood volumes based on reduction factors derived from an extensive empirical database of flood events with LW occurrence (Steeb, 2018; Steeb et al., 2019a, 2022). In Switzerland and other countries around the Alps, some private engineering companies and consultants, specialized on natural hazards, developed their own GIS-based models to estimate the potential LW supply from different recruitment processes (e.g., von Glutz, 2011; Hunziker, 2017).

However, one important aspect of the above-mentioned GIS-based models [10], [5], [12], [11] is that they do not attempt to simulate the actual recruitment processes (e.g., landslides, debris flows, bank erosion), but they used available information on areas susceptible to recruitment processes (e.g., from hazard maps, although these are usually derived from previous modelling studies) or expert-based buffers. An intermediate approach was proposed by Rigon et al. (2012) [19], who applied a geostatistical bivariate analysis (weight of evidence method; Bonham-Carter et al., 1990) to identify unstable areas based on weighting factors. Lucía et al. (2015a) [14] estimated potential LW recruitment in a mountain basin in Italy modelling shallow landslides with a hillslope stability model (Montgomery and Dietrich, 1994) coupled to a connectivity index (Cavalli et al., 2013). The approach was further developed by Franceschi et al. (2019) [15] who used detailed forest information based on a single tree extraction from LiDAR data and combined it with a 1D hydraulic model to evaluate channel widening and LW downstream propagation. Cislaghi et al. (2018) [27] proposed one of the first physically-based stochastic models to simulate shallow landslides combined with the forest stand characteristics to estimate LW recruitment from hillslopes. Similarly, Gasser et al. (2018, 2020) [26] proposed two frameworks to model shallow landslides, and geotechnical and hydraulic bank erosion applying two physically-based stochastic models together with a tree detection algorithm (Dorren, 2017) to estimate LW supply. Zischg et al. (2018) [9] presented a LW recruitment model coupled to a 2D hydrodynamic model to estimate LW recruitment from bank erosion in the flood influence zone of the river. In this approach, wood

168 volumes were also estimated based on a single tree detection algorithm applied to a normalized
169 digital surface model.

170

171 **Table 1: Comparison of published wood supply models. Highlighted in bold: models used for**
172 **comparison in this work, EGA and FGA.**

Spatial scale	Reference	Country	Model name	Processes considered	Temporal scale	Main input variables	Output
Deterministic models							
Stream reach	[1] Rainville et al., 1986	USA (Pacific Northwest)	Not specified	Tree fall	between 25 and 300 years (time steps of 10 years)	Not specified	Number of wood pieces
	[2] Murphy and Koski, 1989	SE Alaska	Not specified	Tree fall and bank erosion	250 years (time steps 1 year)	Survey measurements; channel width, wood diameter, forest stand	Number of wood pieces
	[3] Beechie et al., 2000 (based on Kennard et al., 1999)	USA (WA)	Riparian-in-a-Box	Natural tree mortality, windthrow, bank erosion	150 years (time steps 10 years)	Tree species, diameter, height, and crown ratio in stands; site/reach geometry	Number of wood pieces and LW volume
	[4] Downs and Simon, 2001 (based on earlier models of Simon, 1989 and Hupp and Simon, 1991)	USA (MS)	Simon channel evolution model	Bank erosion and channel avulsion	time steps of 10 years	Channel morphology surveys, rates of knickpoint migration, quantitative characteristics of riparian vegetation	Number of wood pieces and LW volume
	[5] Rimböck, 2001	Germany (Bavarian Alps)	*Luftbildbasierte Abschätzung des Schwemmholzpotenzials LASP* (aerial photo-based estimation of wood potential volume)	Bank erosion, mass failures (i.e., landslides), windthrow, avalanches	Event	DTM, stand density	LW potential volume
	[6] Welty et al., 2002 (same as Kennard et al., 1999 and Beechie et al., 2000)	USA (Pacific Northwest)	Riparian aquatic interaction simulator RAIS	Natural tree mortality, windthrow, bank erosion, mass failures	240 years (time steps 10 years)	Various variables describing forest stand, stream width, initial LW, conifer/hardwood depletion rate, zone widths, windthrow rate, fall direction bias, LW placement option	Number of wood pieces and LW volume
	[7] Benda et al., 2016 (sensu Benda and Sias 2003)	USA (OR)	Reach Scale Wood Model (RSWM)	Tree fall by natural mortality	100 years (5-year time steps)	Stand density, mortality rate, tree height & diameter, slope, stream width	Number of wood pieces and LW volume
	[8] Hassan et al., 2016 (budget concept used in Benda and Sias 2003)	Canada (BC)	Not specified	Tree mortality, bank erosion, mass failures	100 years period	High field data requirements, most can be obtained from air photo measurements, forest inventory data, and/or regional values	LW volume

	[9] Zischg et al., 2018	Switzerland	LWDsimR (coupled with Basement-ETH)	Bank erosion	Event	DEM, hydrograph, forest stand	LW volume
Catchment	[10] Mazzorana et al., 2009	Italy (Autonomous Province of Bolzano)	Not specified	Bank erosion, mass failures, and debris flows	Event	DTM, hazard index map (debris flow, overbank sedimentation), land use map, stand map, torrent network map	Hazard index maps classifying torrent catchments according to a propensity to entrain and deliver LW
	[11] Steeb et al., 2017a, 2019b	**Switzerland (Alps)**	**Empirical GIS Approach (EGA)**	**Bank erosion, mass failures, debris flows**	**Event**	**SilvaProtect-CH data, stream network, catchment area, ecomorphology data, stand data (NFI)**	**Number of wood pieces and LW volume**
	[12] Ruiz-Villanueva et al., 2014c	Spain	Not specified	Fluvial transport, bank erosion and mass failures (i.e., landslides)	Event	DEM, topography, natural hazards maps, geomorphological units, forest density, tree species, height & diameter	Number of wood pieces and LW volume
	[13] Ruiz-Villanueva and Stoffel, 2018	**Switzerland**	**Fuzzy-logic GIS Approach (FGA)**	**Bank erosion, mass failures, debris flows**	**Event**	**SilvaProtect-CH data, stream network, catchment area, DEM, ecomorphology data, stand data (NFI)**	**LW volume**
	[14] Lucía et al., 2015a	Italy (North-western Apennines)	Not specified	Bank erosion, mass failures	Event	DTM, DSM (digital surface model)	LW volume
	[15] Franceschi et al., 2019 (based on the model developed by Lucía et al. 2015)	Italy (South Tyrol)	Not specified	Bank erosion, mass failures	Event	DTM, geomorphological map, precipitation, discharge	LW volume
Both stream reach and catchment	[16] Benda and Sias, 2003	USA (Pacific Northwest)	Not specified	Episodic tree mortality (e.g., fire, wind), bank erosion, mass failures, and debris flows	800-1800 years (time steps 10 years)	Stand density, tree height, channel width, recruitment area & rates	Number of wood pieces and LW volume
	[17] Benda et al., 2007	USA	NetMap	Hillslope erosion, sediment, and wood supply	Not specified	Base terrain parameters including DEM and climate data	LW accumulation type
	[18] Kasprak et al., 2012	USA (ME)	Not specified	Bank erosion, mass failures, and debris flows	100 years period	Stand data, LiDAR DEM	Number of wood pieces
	[19] Rigon et al., 2012	Italy (Eastern Alps)	Not specified	Mass failures (i.e., landslides)	Event	Landslide and debris flow inventory data, stand data, DEM	LW volume
	[20] Benda and Bigelow, 2014 (same model as Benda and Sias, 2003)	USA (CA)	Not specified	Tree mortality, bank erosion, mass failures, debris flows and snow avalanches	100 years period	Survey measurements	wood recruitment, storage and transport
Stochastic models							
Stream reach	[21] Van Sickle and Gregory, 1990	USA (OR)	Not specified	Tree fall	time steps of 10 years	Riparian stand density, tree height, stream length	Number of wood pieces

	[22] Malanson and Kupfer, 1993	USA	FORFLO model	Tree fall	500 years (time steps 1 year)	Tree species, tree height, diameter, water level	Biomass
	[23] Bragg, 2000	USA (Inter-mountain West)	CWD model (1.2)	Episodic tree mortality (spruce beetle outbreak, moderately intense fire, and clear-cut)	300 years (time steps 10 years)	Stand density, species, tree height & diameter	Number of wood pieces and LW volume
	[24] Meleason et al., 2003	USA (Pacific Northwest)	Streamwood	Tree fall by natural mortality	500 years (time steps 10 years)	List of trees that died in a year (wood model input = forest model output)	Number of wood pieces and LW volume
	[25] Eaton et al., 2012	British Columbia	The reach-scale channel simulator (RSCS) was	Tree fall by natural mortality	One-year time step	Tree height, tree diameter, tree fall orientation, forest density, chronic mortality, decay and breakage	Wood load ($m^3 \cdot m^{-2}$) and jam formation
	[26] Gasser et al., 2018 and 2020	Switzerland	SlideforMAP, BankforMAP, FINT	Bank erosion, mass failures	Event	DTM, DSM, precipitation maps, soil map, vegetation efficiency (erosion prevention)	LW volume
Catchment	[27] Cislaghi et al., 2018	Italy (Eastern Alps)	Probabilistic PRIMULA model and a hillslope-channel transfer mode	Mass failures (i.e., landslides)	Event	DEM, geological map, rainfall, forest stand characteristics	LW volume
Empirical models							
Catchment	[28] Rickenmann, 1997	Switzerland, Japan, USA	Not specified	Wood export, (recruitment process not specified)	Event	Catchment area, forested catchment area, stream length, forested stream length, peak flow, flood runoff, and bedload volume	LW potential (instream wood), estimated LW supply volumes
	[29] Steeb et al., 2017b; Steeb, 2018 (updated from Rickenmann, 1997)	Switzerland, Italy, France, Germany Japan	Not specified	Wood export, (recruitment process not specified)	Event	Catchment characteristics, flood event characteristics	LW volume

173

3 GEOSPATIAL MODELLING OF LARGE WOOD SUPPLY IN SWISS MOUNTAIN CATCHMENTS

3.1 General concept

In this contribution, two LW models were compared; the empirical GIS approach (EGA) by Steeb et al. (2017a, 2019b) and the Fuzzy-Logic GIS approach (FGA) by Ruiz-Villanueva and Stoffel (2018) which is a variation of the model presented by Ruiz-Villanueva et al. (2014c). Both, the EGA and FGA are based on a similar general concept (Figure 1) and fed with similar input data and defined equivalent scenarios (see following subsections) to make comparison possible. Both models were developed in the context of *WoodFlow*, a Swiss research program aimed at creating knowledge and methods to analyse instream wood dynamics, with particular attention to watercourses in the Alpine region (FOEN, 2019).

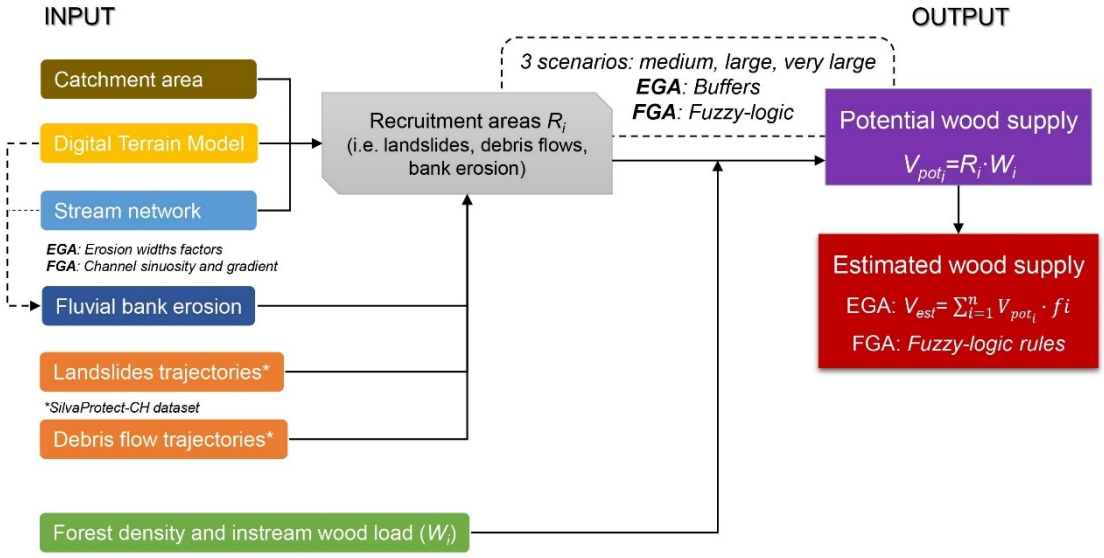

Figure 1: Conceptual model of the empirical GIS approach (EGA) and the Fuzzy-Logic GIS approach (FGA). V_{pot} = potential wood supply [m^3]; V_{est} = estimated supplied wood [m^3]; i = recruitment process [-]; R = recruitment area [ha]; W = forest density or instream wood load [m^3 ha^{-1}]; f = volume reduction factor [-]. Three different scenarios were defined (see section 3.5): medium scenario (medium-to-high frequency and intermediate magnitude), large scenario (relatively low frequency and medium-to-high magnitude), and very large scenario (very low frequency and very high magnitude).

The general concepts and main steps of the GIS-based approaches were to (i) identify the recruitment areas on the hillslopes and along the stream network that may contribute woody material to streams, such as areas affected by landslides, debris flows and bank erosion; (ii) create three different scenarios based on the process frequency and magnitude; and to (iii) provide estimates of potential LW supply V_{pot} (i.e., worst case scenarios) and supplied wood volumes for each scenario V_{est}. The methods aim at estimating supply wood volumes at the catchment scale and do not include the analysis of wood transfer (i.e., transport and deposition) through the stream network.

Potential large wood supply V_{pot} was calculated by intersection of the modelled recruitment areas with forest cover. During a flood, however, only a part of the LW potential is actually recruited and exported out of the catchment. Therefore, empirically derived volume reduction factors (EGA) or fuzzy logic principles (FGA) were applied to best estimate actual supplied LW volumes V_{est}. Modelling results were validated by comparison with available empirical data documented after flood events in Switzerland (Steeb et al., 2021, 2022). This dataset documents recruited and transported quantities of large wood together with the associated catchment and flood-specific parameters, including the associated recruitment processes (Table S1 in supplementary material).

3.2 Input data

3.2.1 Catchment areas and stream network

The topographical catchment areas (feature polygons), which define the perimeters of investigation, were available from the geodataset "topographical catchments of Swiss waterbodies" (FOEN, 2015). The stream network of Switzerland at a scale of 1:25,000 (swissTLM3D, © 2016 swisstopo [DV033594]) was pre-processed by adding information on channel width as derived from a Swiss-wide ecomorphological dataset (Ökomorphologie Stufe F ©FOEN; Zeh Weissmann et al., 2009). Based on this dataset, the channel width was

known for 42 % (25,800 km) of the total Swiss streams' length. For the remaining 58 %, we extrapolated channel width based on stream order (Strahler, 1957) and altitude classes (Table S2).

The stream network and channel widths were used to define intersections and connectivity between the hillslopes processes and the streams, to estimate the bank erosion prone areas (sections 3.3 and 3.4) and to assign values of instream dead wood volumes (section 3.2.3).

3.2.2 SilvaProtect-CH and the identification of landslide and debris flow trajectories

For the modelling of the two recruitment process categories landslide and debris flow, both GIS models used the SilvaProtect-CH dataset from Losey and Wehrli (2013). As part of the SilvaProtect-CH project, several natural hazard processes were modelled over the entire Swiss territory using partly physically-based models. As a result, process trajectories that describe the topographic flow path and runout distances (from starting to deposition zone) of the investigated natural hazard processes were readily available (details are provided in the supplementary material). These trajectories were processed further to identify potential recruitment areas of LW supply (sections 3.3. and 3.4).

3.2.3 Forest density and instream wood load

The density of living trees in Swiss forests [m^3 ha^{-1}] was derived from a Swiss nationwide raster map with an original resolution of 25 x 25 m (rescaled to 1 x 1 m; Figure 2). The raster map is based on a growing stock model developed by Ginzler et al. (2019) that quantifies forest density in relation to tree height (based on airborne stereo imagery), canopy cover, topographic position index, mean summer temperature and elevation. The EGA and FGA models further consider an estimate of deadwood on the forest floor [m^3 ha^{-1}] (i.e., equal to 5% of living trees density) based on empirical data of the Swiss National Forest Inventory (NFI; WSL, 2016).

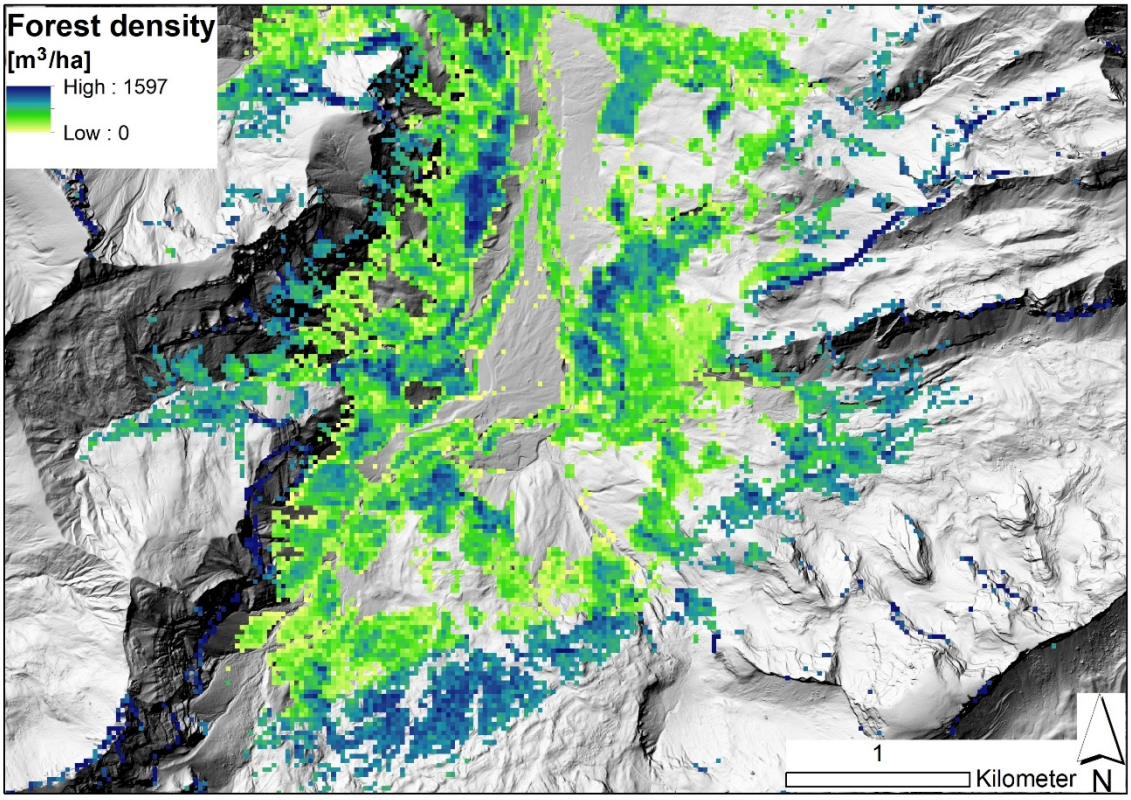

Figure 2: Example of the wood stock raster map in the Grosse Melchaa catchment near Stöckalp (Canton Obwalden). Background: Digital terrain model (hillshade), © swisstopo.

Additionally, instream wood loads were included in the calculations, accounting for potential LW volumes from accumulated deadwood in the channel. Detailed information on wood loads across the stream network was not available, so based on a literature review by Rickli and Bucher (2006) and Ruiz-Villanueva et al. (2016), volumes of instream wood were assigned to the different streams grouped by channel width (EGA) or by stream order (FGA) classes (see following sections).

3.3 The empirical GIS approach (EGA)

Debris flow and landslide trajectories from SilvaProtect-CH were constrained by intersection with the stream network and forest cover. Only landslide trajectories with starting points within a 50-m distance from the stream network were considered. This limitation was supported by the landslide database of Rickli et al. (2016) where 44 % of all documented landslides showed a runout distance of less than 50 m (around 80 % are within a distance of 100 m). For each scenario (section 3.5), different buffer widths w_b were applied on both sides of the relevant debris flow and landslide trajectories (i.e., medium scenario: w_b = 5 m; large scenario: w_b = 10 m; very large scenario: w_b = 15 m). The buffer widths were chosen in ranges according to the Swiss landslide database (Rickli et al., 2016). Potential recruitment areas were finally extracted as the overlap of the buffered trajectories with the forest layer.

The extent of bank erosion in EGA was assumed to be proportional to the given channel width. Scenario-specific erosion width factors e_w (i.e., a multiple of the channel width) were empirically derived from observations after the well-documented August 2005 flood in Switzerland, for which a large dataset was analysed and made available (Bachmann Walker, 2012; Hunzinger and Durrer, 2008). Scenario-specific erosion width factors were e_w = 1.5 for the medium scenario, e_w = 3 for the large scenario, and e_w = 4.5 for the very large scenario. The resulting buffer widths were added to the original channel width. Potential recruitment areas due to bank erosion were finally extracted as the overlap of the buffered stream network with the forest layer.

The estimation of previously stored wood load within the river network (i.e., instream deadwood) was based on empirical values of wood storage per stream hectare. Rickli et al. (2018) documented instream wood storage for ten reaches in Swiss torrents. This database was complemented with 39 additional values from various other European rivers, based on a literature review by Ruiz-Villanueva et al. (2016), in order to have reliable derivations. Finally, we assigned wood load values into three channel width classes (i.e., <5 m = 94 $m^3 \cdot ha^{-1}$; 5-10 m = 67 $m^3 \cdot ha^{-1}$; >10 m = 42 $m^3 \cdot ha^{-1}$).

283 Potential source areas from different recruitment processes may partly overlap. For this
284 reason, a priority sequence was determined so that such overlapping areas were not counted more
285 than once. This was defined according to the following principle: The closer to the channel a
286 recruitment process occurs, the higher the priority: instream wood > debris flow > bank erosion
287 > landslide. For example, overlapping areas of debris flows and bank erosion were assigned to
288 the process area debris flow.

289 Potential recruitment areas were finally used to calculate the potential LW supply V_{pot} by
290 multiplying the process areas with the respective forest density (for debris flows, landslides, and
291 bank erosion) or wood load (for instream deadwood). From the resulting potential LW supply,
292 the actual LW supply V_{est} was estimated. To do so, volume reduction factors f were used, which
293 assumed different values depending on the recruitment process and scenario of process magnitude
294 (Table 2). The volume reduction factors were empirically determined with three different
295 approaches (Steeb et al., 2019b): 1) Comparison with literature data, including values from other
296 studies and models that proposed reduction factors; 2) comparison of potential vs. observed
297 recruitment areas; and 3) comparison of estimated vs. observed wood volumes in well
298 documented catchments during the 2005 flood (see the five blue catchments in Figure 3).

299 Values of observed LW supply volumes and recruitment areas together with the associated
300 catchment and flood specific parameters were taken from a complementary empirical dataset that
301 was also part of the WoodFlow research program. In total, the LW database consisted of 210 data
302 entries. Most entries (171) refer to events in Switzerland. Also included are flood events from
303 Japan, Italy, Germany and France (Steeb et al., 2019a).

304

Table 2: Overview of volume reduction factors *f*, classified by scenario and recruitment processes.

Scenario	Instream wood	Debris flow	Bank erosion	Landslide
Medium	0.10	0.05	0.05	0.01
Large	0.30	0.10	0.10	0.05
Very large	0.70	0.30	0.20	0.10

The EGA model has been originally developed with ArcGIS 10.1 (©ESRI) and updated with ArcGIS 10.8 (©ESRI). The toolbox is freely available for download on the website *www.woodflow.ch*.

3.4 The Fuzzy-Logic GIS approach (FGA)

The areas prone to landslides and debris flows were defined based on the linear trajectories provided by the SilvaProtect-CH database. To transform these lines into areas (i.e., pixels, as the FGA is entirely raster based), the density of the lines was used to classify the terrain into three intensity scenarios (section 3.5). High trajectory density was assumed to represent areas that are more prone to landslides or debris flows, more likely of a higher frequency and therefore, lower magnitude. Low trajectory density was assumed to represent areas that are less prone to mass movements, more likely affected by higher magnitude and thus lower frequency events. The thresholds to classify the three areas was based on four natural breaks (Figure S1A in supplementary material). In the case of mass movements, the delivery of wood to the stream network depends not only on the area of the landslide, but also on its connectivity to the channel (Ruiz-Villanueva et al., 2014c). Once the trajectories were converted to density pixels, the connectivity between these pixels and the stream network was established for landslide-prone pixels, as a function of both the distance to the channel and the terrain slope. In addition, a buffer area of influence was also established around these areas, to include toppled trees that may be recruited indirectly by the action of landslides. Trees located in a landslide-prone pixel or in the

328 toppling influence area (defined as a buffer equal two times the mean tree high; here 100 m), may
329 reach the channel if they were close enough (Euclidean distance to channel network < 50 m) or
330 further away (Euclidean distance up to 100 m) but on a steep slope (>40%;). In the case of debris
331 flows, all pixels were assumed to be connected to the stream network.

332 Areas prone to bank erosion were computed based on channel sinuosity and gradient (as
333 proxies for channel lateral migration and transport capacity; Ruiz-Villanueva et al., 2014c), the
334 channel width and a defined width ratio. The width ratio was used to estimate the potential
335 resulting channel width after bank erosion during floods. It was calculated analysing an European
336 database (Ruiz-Villanueva et al., *in prep.*), including several rivers and flood events in
337 Switzerland and other 6 countries, and three scenarios were defined for different channel width
338 classes (9 classes ranging from < 3 to > 50 m). The stream network provided by the
339 ecomorphology database (section 3.2.1) was grouped by the channel width classes considered and
340 the width ratio was assigned to estimate the resulting potential erodible width for each stream
341 segment (Figure S1). The width ratio (ranging between 1 and 4) generally increases with scenario
342 intensity and decreasing channel width. The resulting buffers were transformed to pixels and the
343 final pixels prone to bank erosion were assigned based on channel sinuosity and gradient. Stream
344 segments characterized with high sinuosity and high gradient were assumed to be more prone to
345 bank erosion.

346 The described variables (i.e., landslide prone areas, connectivity, debris flow prone areas,
347 bank erosion prone areas, sinuosity and gradient) were transformed to fuzzy sets using the Fuzzy
348 Membership tool initially developed in ArcGIS 10.1 and updated to ArcGIS 10.7 (©ESRI) with
349 a linear membership function. The resulting converted fuzzy variables were combined (e.g.,
350 landslides prone pixels and connectivity; sinuosity and gradient) with the Fuzzy Overlay tool
351 (©ESRI). As a result, all pixels were transformed to fuzzy values ranging from 0 to 1; they were
352 then used to compute the volume of wood by multiplying the fuzzy pixel value by the forest
353 density pixel value (section 3.2.3). In case of overlaping pixels, priority was given to areas prone
354 to debris flows, then bank erosion and finally landslides (as in the EGA approach). The final

calculation considered also the accumulated wood load within the river network, but applying a slightly different approach than for the EGA. This was estimated by assigning wood load values based on the literature (Ruiz-Villanueva et al., 2016) to the different river segments grouped by stream order classes following the approach of Wohl (2017) (i.e., < 3 stream order: 60 $m^3 \cdot ha^{-1}$; between 3 and 6 order: 120 $m^3 \cdot ha^{-1}$; > 6 order: 50 $m^3 \cdot ha^{-1}$) and multiplied by fuzzy layers.

3.5 Model scenarios definition

Three different scenarios were designed to estimate supplied wood volumes, based on a qualitative assessment of the frequency and intensity of the wood recruitment processes involved. These scenarios are called: medium scenario (medium-to-high frequency and intermediate magnitude), large scenario (relatively low frequency and medium-to-high magnitude), and very large scenario (very low frequency and very high magnitude).

Most of the documented floods with LW occurrence that were used to validate the GIS models had a precipitation and/or peak runoff return period of 50-150 years, which was assigned to the large volume scenario. The other two scenarios refer to approximate return periods and were determined using *ad hoc* volume reduction factors (EGA) or the fuzzy logic rules (FGA), because they could not be quantified more precisely due to a lack of data.

In addition to the estimated supplied wood volumes for each scenario, a potential wood volume was also computed. The potential volume was assumed to be the maximum wood volume supplied at the catchment scale, computed without any reduction by a coefficient (EGA) or by the fuzzy logic values (FGA).

3.6 Test catchments

In the 40 catchments analysed in this work (Figure 3), considerable amounts of LW were recruited and transported during past floods, and the resulting LW volumes were well documented (mainly from the August 2005 flood; Rickli et al. 2018 and Steeb et al., 2017b). Table S1 in the supplementary material provides an overview of the 40 test catchments and their characteristics.

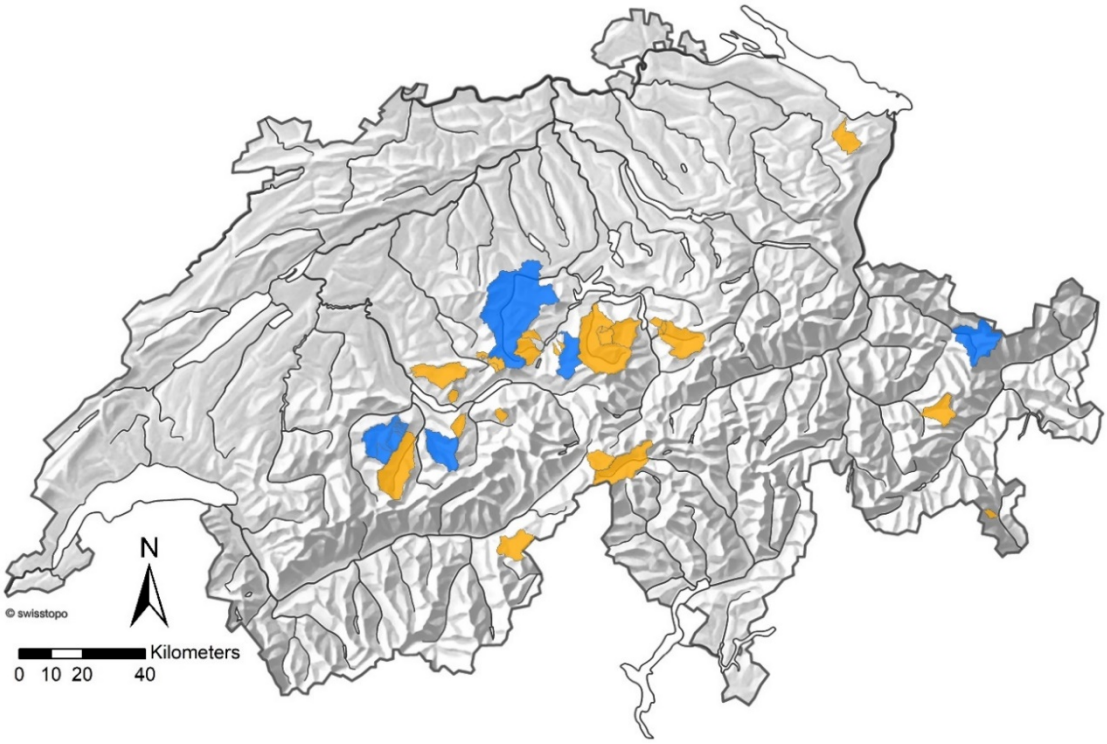

Figure 3: Location of the 40 test catchments (orange; with many nested sub-catchments). The five catchments in blue (Chiene, Chirel, Grosse Melchaa, Landquart, Kleine Emme) were used to calibrate the volume reduction factors from the EGA approach so that the estimated supplied wood was in the same order of magnitude as the observed values from past flood events.

3.7. Model results analysis

Model results were first compared to observed wood volumes during floods, and then analysed in terms of (modelled) wood volumes per scenario, potential wood volume, wood volume supplied by different recruitment or supply processes (i.e., landslides, debris flows and bank erosion), and the estimated instream wood volume.

Statistical analyses were realized with the software RStudioVersion 2021.9.0.351 (R Studio Team, 2021). Differences between the two models and between them and the available observations were analysed in terms of mean values, standard deviation (SD) and root mean square error (RMSE), and tested by the nonparametric Wilcox (Mann-Whitney) or Kruskal-Wallis tests for two or more groups respectively (Stats package; R Core Team, 2019). Differences in the distributions of observed versus estimated wood supply volumes ('large' scenario) were tested using the Kolmogorov-Smirnov Test. Significance was set to a p value <0.05. The dependence of wood volume on catchment controlling variables was verified by means of scatter plots, regression analysis and correlation (*ggally* package; Schloerke et al., 2021).

4 RESULTS

4.1 Comparison between model outputs and model approaches (EGA/FGA)

The two GIS approaches provide geospatial outputs – EGA in the form of feature class polygons and the FGA in pixel-based raster files – that can be visualized on a map, as shown in Figure 4. Potential recruitment areas for debris flow, landslide and bank erosion are generally larger for EGA, i.e., the defined EGA buffer widths provide more supply-prone areas than the respective combination of FGA fuzzy layers within the same perimeter.

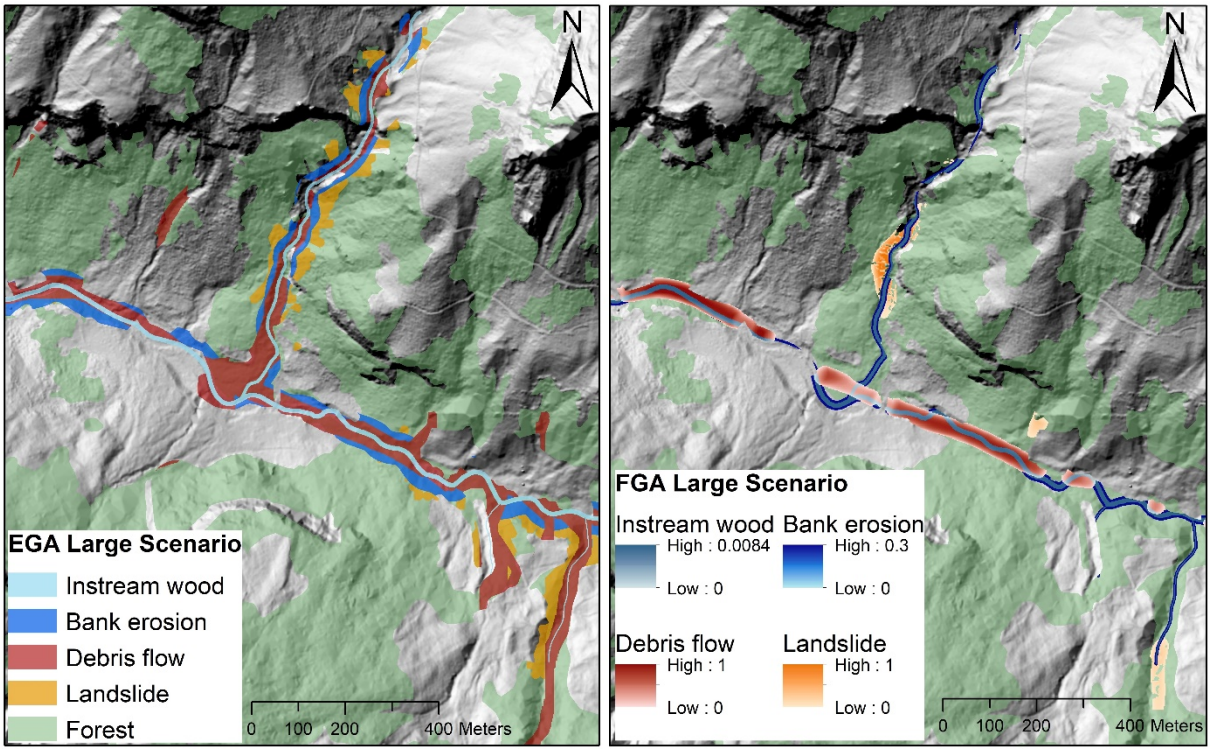

Figure 4: Large volume scenario comparison of model outputs from EGA (left) and FGA (right) at the Spiggebach torrent within the Chiene river catchment (Canton Bern). Potential recruitment areas are shown for landslides (orange), debris flows (red), and bank erosion (dark blue). The stream network (light blue) includes also instream wood loads. Background: Digital terrain model (hillshade), © swisstopo.

The estimated supply and potential wood volumes for the three scenarios and the two models are shown in Figure 5 together with the available observations. The comparison between modelled and observed wood volumes is presented in section 4.3, the focus here is on differences between the two models. In general terms, Figure 5a highlights that the estimated supply wood volumes for each scenario were larger when computed by the FGA and lower by the EGA. For example, for the medium scenario, the averaged wood volumes were 994 m^3 and 3318 m^3 for EGA and FGA, respectively. The differences were slightly reduced for the other two scenarios, for which volumes equal to 7127 m^3, 17353 m^3, 8199 m^3 and 19712 m^3 were obtained (for the large and very large scenarios and the EGA and FGA, respectively; Table 3).

The variation in estimated wood supply is similarly high for both models, as shown by the statistical values in Table 3. Except for the maximum value of the 'very large' scenario, FGA has generally slightly larger percentile values. The standard deviation for the 'large' scenario is 20260 for EGA, and 20792 for FGA. The estimated wood supply volumes of EGA and FGA correlate well with only narrow scattering (Figure S6A), and the residuals increase similarly with increasing catchment size (Figure S6B).

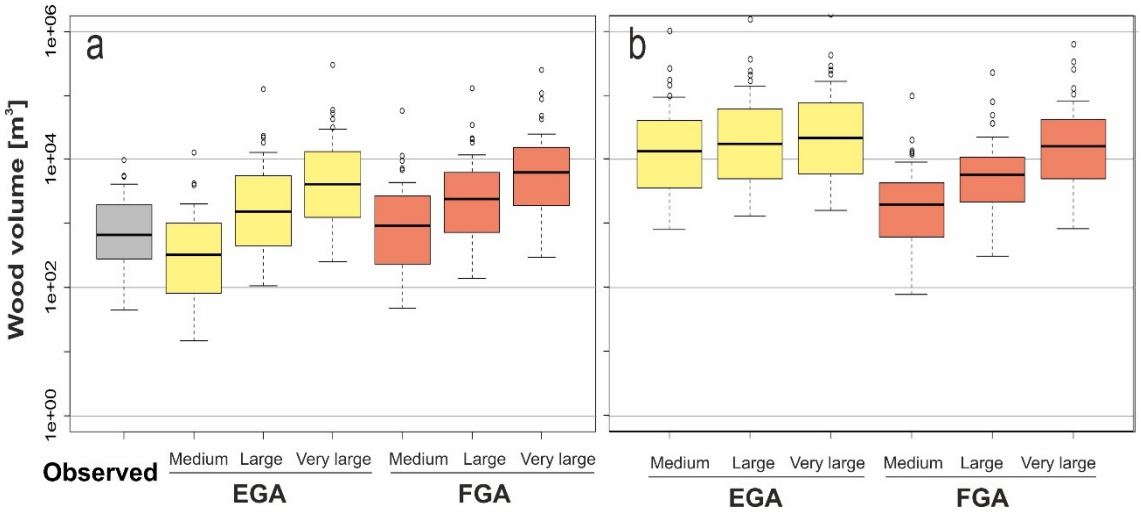

Figure 5: Boxplots of wood supply (a) and potential (b) volume (m^3) estimated by the two models EGA and FGA, and the three scenarios (i.e., medium, large, very large). "Observed" refers to the reported LW volumes after flood events (n=40; shown in grey colour), in most cases equivalent to the large scenario.

Table 3: Statistical values of observed and estimated LW supply volumes for the three scenarios (i.e., medium, large, and very large) and the two models (i.e., EGA and FGA) for all studied catchments. "Observed" refers to the reported LW volumes after flood events, in most cases equivalent to the large scenario.

Wood supply volume [m^3]	Observed	EGA			FGA		
		Medium	Large	Very large	Medium	Large	Very large
Min.	45	15	106	253	48	141	300
1st	290	83	475	1378	244	764	2037
Median	673	329	1562	4189	921	2430	6342
Mean	1428	994	7127	17353	3318	8199	19712
3rd	1906	967	5161	12609	2588	6083	15191
Max.	9741	12757	126648	296893	57152	128575	249256
Standard deviation (SD)	1927	-	20260	-	-	20792	-
Root Mean Squared Error (RMSE)	-		20225	-	-	21052	-

Significantly higher values were computed for the large and very large scenarios compared to the medium scenarios, with a similar pattern shown by the two models. Larger differences were observed when comparing the estimated potential volumes (Figure 5b and Table 4). In this case the EGA resulted in much higher values than the FGA (especially for medium and large scenarios), which is a result of much larger potential recruitment areas (Figure 4) Accordingly, the percentile values of EGA potential LW supply volumes show more variability. Figure S3 shows that for EGA, the estimated LW supply volume corresponds to 8 % of the potential wood supply volume on average. In the case of FGA, this ratio varies much more with an average of 47 %.

Table 4: Potential LW supply volumes for the three scenarios (i.e., medium, large, and very large) and the two models (i.e., EGA and FGA) for all studied catchments.

Potential wood volume [m^3]	EGA			FGA		
	Medium	Large	Very large	Medium	Large	Very large
Min.	807	1289	1601	76	305	811
1st	3529	4949	6000	613	2203	5341
Median	13226	17579	21619	1965	5774	15965
Mean	58664	86984	105723	5961	16173	52995
3rd	37672	59612	74948	4207	10665	41066
Max.	1011306	1534850	1866295	100165	231336	632151

4.2 Contribution from different supply processes

The main difference between the two models was the estimated contribution from each supply process to the obtained wood volume. Landslides were the dominant process in the case of the EGA, with a contribution up to more than 60% of the computed wood volume (for the large scenario); whereas bank erosion was the predominant process in the FGA model for all scenarios (Figure 6). Debris flows played an intermediate role in supplying wood according to the two models; however, the importance of this process varied depending on the scenario. For the medium scenario, the EGA model showed a similar percentage of averaged wood supplied by landslides and debris flows. The FGA, contrastingly, computed most of the averaged wood volume supplied by bank erosion, and only a low percentage of wood supplied by landslides and debris flows. Only for the very large scenario, the importance of landslides, in terms of percentage of supplied wood, equalled or even exceeded, the volume estimated from bank erosion with the FGA.

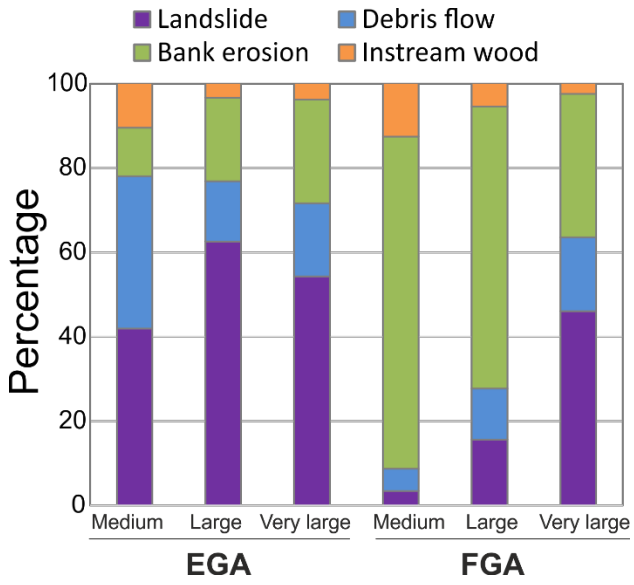

Figure 6: Large wood volumes supplied by each process, model, and scenario averaged for all 40 study sites.

The difference between the contribution of each process to the estimated volumes is clearly shown in Figure 7 and 8 (with FGA resulting in generally higher volumes than EGA). The graph illustrates that statistically significant differences were found between the computed supply wood

volumes by the two models and by bank erosion process. The median wood supply values (see black lines within boxplots of Figure 7) are about a factor of 1000 and 10 larger for the FGA than for the EGA, and for the medium and large scenarios respectively. This explains the relative dominance of bank erosion for the FGA (see also Figure 8), for the medium and large scenario. The wood volumes supplied by the other processes were not significantly different between the two models. Only the estimated instream wood volume for the medium scenario showed a significant difference between the EGA and the FGA, with larger volumes computed by the latter.

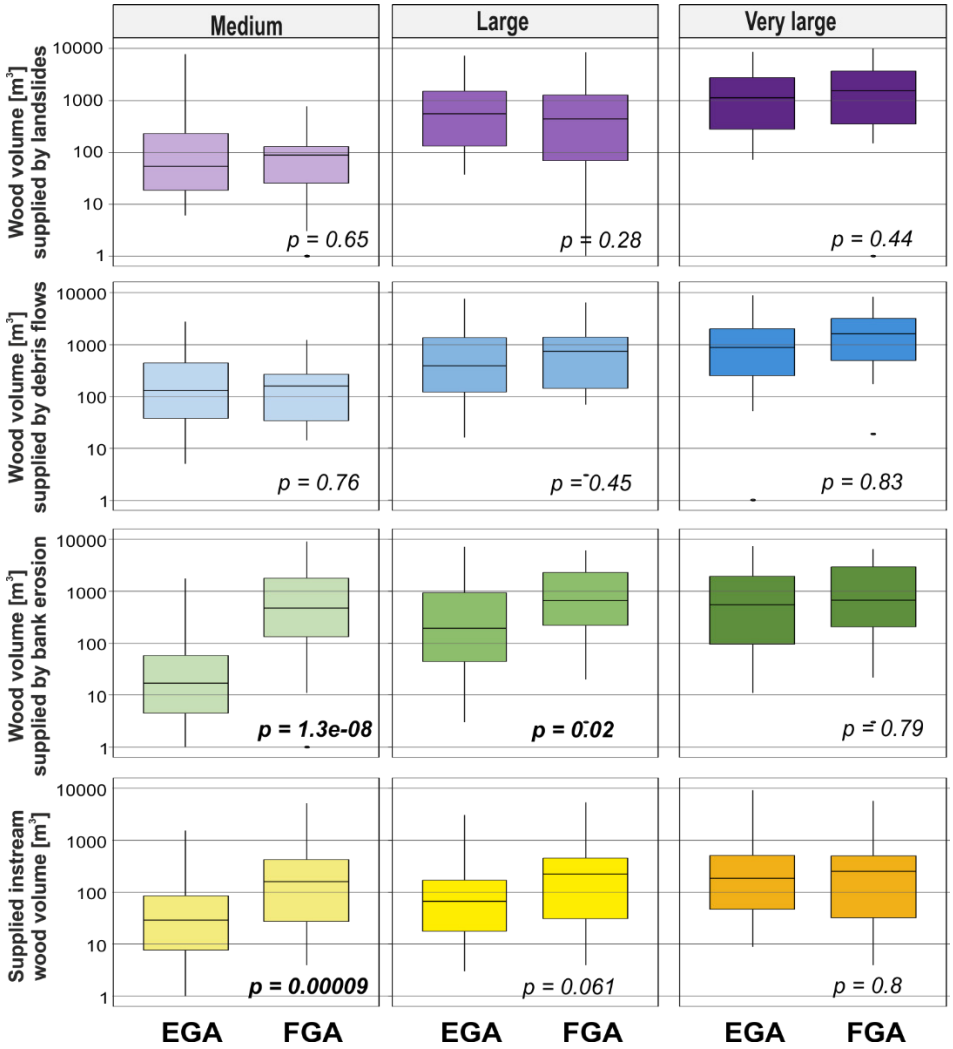

Figure 7: Wood volumes supply estimated for landslides, debris flows, bank erosion, and estimated supplied instream wood by the two models and the three scenarios. The p-value is from the Wilcoxon test (significant values shown in bold).

However, the contribution of each process to the computed wood volume did not only vary according to the model, but also according to the site. Figure 8 shows a selected sub-dataset of catchments with different drainage areas, revealing the large variability of the dominant wood supply process, and the dominance of different processes over the others in the two models. In general, the FGA approach shows a larger contribution from landslides and debris flows in smaller catchments, while landslides are the major contributor to wood supply regardless the catchment size for the EGA. Bank erosion is a minor contributor to the estimated supply in EGA for most sites and irrespective of the scenario used. However, bank erosion is the most relevant process for the FGA, which is clearly illustrated by the Kleine Emme River catchment, the largest of the study sites of the dataset, for which the FGA estimates the largest contribution by this process. The EGA model, on the other hand, estimated a larger contribution from landslides for this site.

The proportion of instream wood loads remains constant, independent of catchment size (2-13 % of total wood supply). The contribution of debris flows and landslides are highly variable depending on topography, and can be dominant for small (e.g., Secklisbach) or large catchments (e.g., Grosse Melchaa or Chirel).

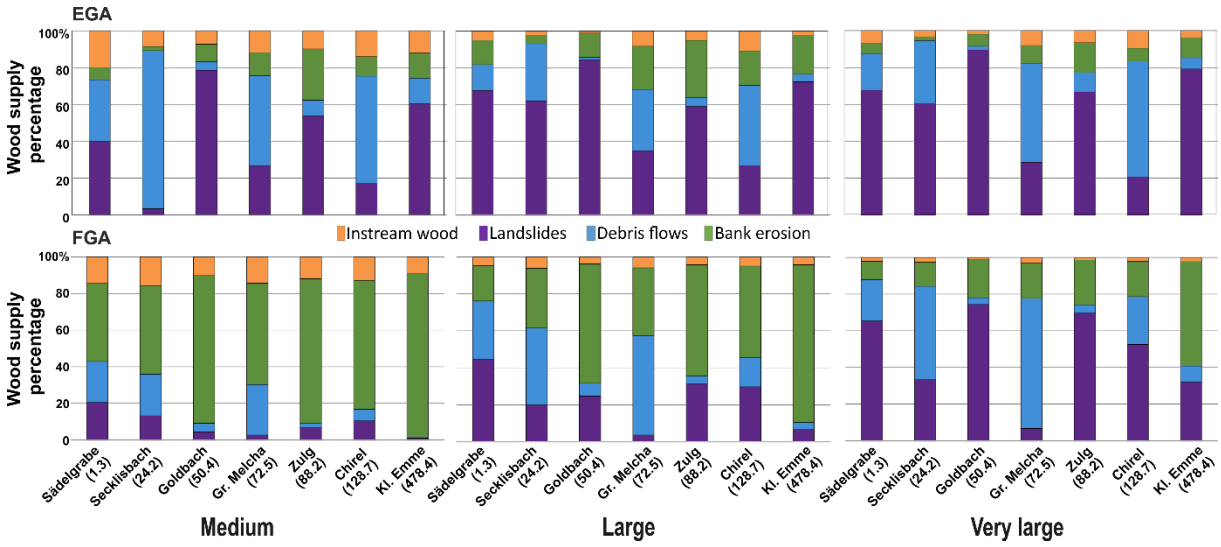

Figure 8: Percentage of wood volume supplied by each process, model, and scenario for selected studied sites, the names and catchment area in (km^2) are provided in the abscissa.

4.3 Estimated and observed wood volumes

The comparison between observed LW volumes V_{obs} and estimated (modelled) LW volumes V_{est} are shown in Figure 9a. There is a relatively large scattering when comparing observed and estimated wood loads. Both under- and overestimation of V_{obs} are observed for both models, with a larger tendency for overestimation. Overestimation remains generally within two orders of magnitude (typically higher values for FGA), underestimation within one order of magnitude (typically lower values for EGA).

Figure 9b further shows the ratio of V_{est}/V_{obs} vs. catchment area. Both under- and overestimation of V_{obs} are present over >2 order of magnitude for all catchment areas. However, in general, overestimation increases with increasing catchment size for both models. There is a shift around a catchment area of 7 km^2, above which overestimation is significantly larger (with a factor of >10). In catchments with areas less than 7 km^2, estimated wood supply is generally underestimated (see dashed line in Figure 9b).

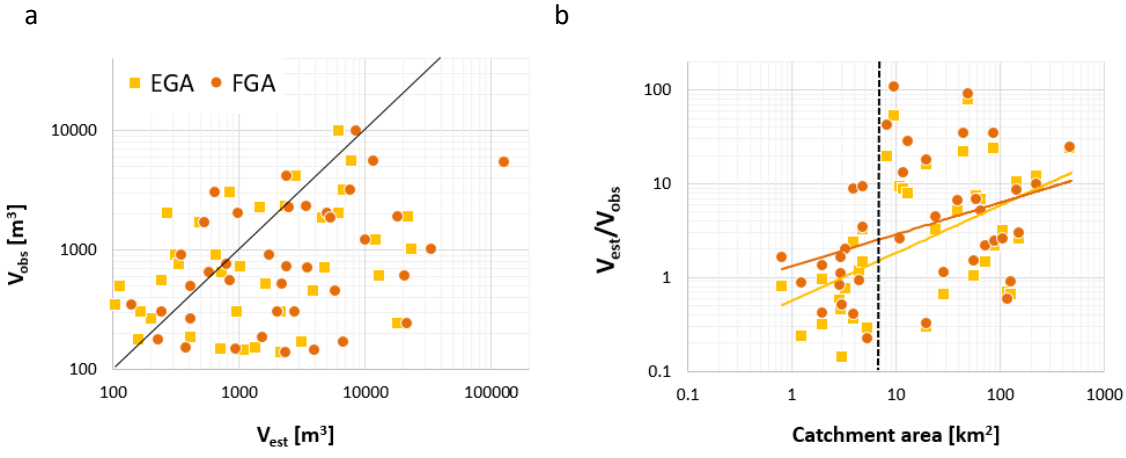

Figure 9: Left: Modelled LW V_{est} (large scenario) versus observed wood volume V_{obs} during past events. The black line shows the line of equality (1:1 line). Right: Ratio of V_{est}/V_{obs} versus catchment area.

This tendency of overestimation with increasing catchment size can also be explained by comparing the ratio of observed and potential wood volume V_{obs}/V_{pot} versus catchment area (Figure 10a). With increasing catchment size, there is a trend of decreasing ratio values of V_{obs}/V_{pot}. This means in larger catchments, the volume reduction factors (FGA) and the fuzzy rules

(FGA) are often not small enough to reduce the wood potential accordingly, creating overestimation of wood volumes ($V_{est} > V_{obs}$).

Since potential wood volumes are much higher for EGA (Table 4 & Figure 5b), the ratio of V_{obs}/V_{pot} is also much smaller in case of EGA (almost one order of magnitude difference as shown in Figure 10b). For FGA few examples (i.e., six orange dots in Figure 10a) exist for which the potential wood volume is even smaller than the observed wood volume ($V_{obs}/V_{pot} > 1$).

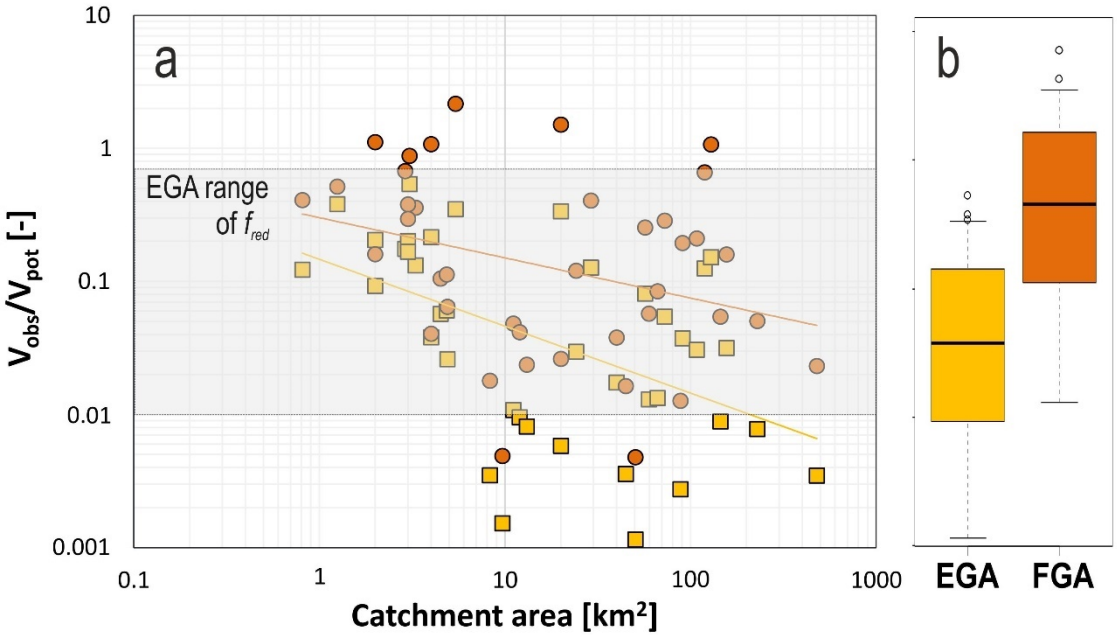

Figure 10: Ratio of observed wood volumes and potential wood volumes computed by the two models for all sites and their catchment areas. The grey rectangle shows the reduction factor range used for EGA computations.

A statistically different distribution could only be observed for the FGA compared to the observed values. The comparison between the values obtained by the EGA and those observed, and between the values obtained by EGA and those obtained by FGA, showed no significantly different distributions (Table S3). This outcome is also illustrated in the histograms of Figure S7.

5 DISCUSSION

5.1 Major differences between the two models and remaining challenges

Both the EGA and FGA are based on a similar general concept, were fed with similar input data (e.g., stream network, forest density, areas affected by landslides and debris flows) and run with defined equivalent scenarios which made the comparison possible. However, there are also some methodological differences that resulted in different model outputs. Here we describe them, while in the following section we discuss our results comparing them to current knowledge and other existing methodologies.

The most relevant difference between the EGA and FGA is the approach to define the areas affected by **bank erosion**, thus the contribution of this recruitment process and the estimated wood supply volumes. EGA uses buffers around the stream network computed for each scenario with one specific width factor, independent of the original channel width. The resulting buffer widths were added on both sides of the original channel width (section 3.3). FGA also assigned scenario-specific buffers, computed with width ratios that vary according to nine channel width classes (Figure S1). Half of the resulting buffer widths were added on both side of the original channel width. As a result, potential bank erosion recruitment areas are generally larger for EGA than for FGA. However, the reduction factors used for the EGA assumed that between 5% and 20% of the potential wood volume within these areas contribute to the estimated wood supply, which resulted in a much lower estimated wood volume. In the case of the FGA, the entire forested area identified as prone to bank erosion along the river network is contributing to wood supply and the volume is reduced based on fuzzy logic pixel values (computed based on sinuosity and channel slope, and going up to 30% of the potential), which resulted in a much larger volume. This difference is particularly relevant for the medium scenario, for which the bank erosion width identified by both models are quite similar, but the resulted wood volumes significantly differ (e.g., average wood volume equal to 114 and 2613 m^3 for EGA and FGA respectively for all sites). Moreover, the erodibility of the channel banks was not considered in the models. Anthropic elements such as bank protection, check-dams, and bridges or the presence of bedrock may limit

574 bank erosion and widening, and thus wood supply. This information was not available at the
575 required resolution and spatial scale for the catchments analysed, and could therefore not be
576 included. This also results in an overestimation of the computed wood volumes due to bank
577 erosion, which may be more relevant in the FGA than in the EGA (for which the volume reduction
578 coefficient could be more easily adjusted).

579 As shown in section 4.2, landslides are the **dominant recruitment process** in the case of the
580 EGA, whereas bank erosion is the predominant process in the FGA model. In both models, for
581 landslides and debris flows, the input data were the trajectories from the SilvaProtect-CH
582 database, but the EGA applies an expert-based buffer for each scenario to those trajectories, while
583 the FGA groups them in three classes according to their density. In addition, the fuzzy
584 connectivity applied in the FGA further reduces the areas identified as prone to mass movements
585 (only for landslides). This hillslope-channel network connectivity is another methodological
586 difference between the two models. In EGA, as a proxy for connectivity, only landslide
587 trajectories within 50 m distance from the stream network were considered. FGA considers
588 connectivity as a function of both the distance to the channel and the terrain slope (as used by
589 Ruiz-Villanueva et al., 2014c). Noteworthy, both models use Euclidean distance, but no
590 geomorphometric measures (e.g., steepest downslope direction) as often used to assess sediment
591 connectivity (e.g., Cavalli et al., 2013).

592 The EGA generally produces much larger potential recruitment areas for landslides and
593 computes larger wood supplied by landslides than the FGA, for all three scenarios. For the FGA,
594 landslides are minor supplier of wood for the medium and large scenarios, while their contribution
595 for the very large volume scenarios significantly increases.

596 Existing observations show that mass wasting processes, such as debris flows and landslides,
597 often are the most relevant recruitment processes in smaller headwater catchments (e.g., Rigon et
598 al., 2012; Hassan et al., 2016; Seo et al., 2010). In contrast, (lateral) bank erosion is often prevalent
599 farther downstream in larger mountain or lowland rivers, resulting in large volumes of LW supply
600 by this fluvial recruitment process. This was observed after the large flood in 2005 in Switzerland

(Steeb et al., 2017b), the large flood in the Magra River catchment in Italy in 2011 (Lucía et al., 2015c; Comiti et al., 2016) and along the Emme river catchment in 2014 (Ruiz-Villanueva et al., 2018). In smaller streams, bank erosion and channel widening can also be significant, especially in natural reaches (no stream regulation works), as seen after severe flash floods in Braunsbach, Germany in 2016 (Lucía et al., 2018). In most of these cases, only a small proportion (<30%) of the total recruited wood was supplied by mass wasting processes, and the majority of the supply was due to bank erosion and channel widening along the river network.

Such catchment size-specific trends of dominant recruitment processes are not clearly prevalent in the model results of EGA and FGA. Generally, the variability in the recruitment processes and thus in the wood supply is very large, both in empirical data as well as in modelling results, highlighting the importance of other catchment- and event-specific characteristics. The relationship of estimated LW supply with catchment characteristics is shown in supplementary material Figure S2. The highest correlation is seen for forested stream length that can be interpreted as a proxy for potential supply volume for bank erosion. High correlations also exist for Melton ratio and relief ratio, both surrogates for watershed slope, a factor that is directly related to stream power and debris flow and landslide propensity. In general, V_{obs} from EGA shows slightly higher correlations (R^2) with catchments characteristics than FGA. More research is needed to better understand wood recruitment processes and to improve predictive models on a physical basis. This will help to determine where and how likely mass wasting (landslides) or bank erosion could occur.

The results in section 4.3 indicate that there is both under- and overestimation of wood supply volumes. As shown in Figure S4, potential LW supply V_{pot} generally increases with catchment size. During a convective storm event, often only a part of the catchment is affected, and therefore geomorphologically active, so that LW supply may easily be overestimated ($V_{est} > V_{obs}$). In smaller catchments and torrents, sporadic recruitment processes such as landslides or debris flows can dominate and deliver large amounts of wood at once, so that wood supply may be underestimated by our models ($V_{est} < V_{obs}$).

628 Another important aspect regarding the overestimation of the calculated wood volumes by
629 the FGA and EGA is the assumption that the estimated volumes are supplied and exported to the
630 outlet of the catchment, which may not be the case if the wood is being deposited along the way.
631 The models do not consider the transfer of the wood along the river network (as, for example, in
632 the approaches of Franceschi et al., 2019 or Zischg et al., 2018).

633 A less relevant difference between the models, and in terms of the total contribution to the
634 wood volume estimations, is the approach used to assign previously **deposited instream wood**
635 **loads**. The EGA assignes instream wood load values into three channel width classes (section
636 3.3), whereas FGA assignes wood load values into three stream order classes (section 3.4). The
637 main divergence comes from the assumption that the smaller channels contain the largest instream
638 wood load for the EGA (following observations in 10 small mountain streams in Switzerland
639 from Rickli et al., 2018), while the FGA assumes that larger loads are present in medium order
640 channels (as proposed by Wohl, 2017). Despite the different approaches, both models used
641 empirical data from Ruiz-Villanueva at al. (2016) to assign volumes, and the resulting wood load
642 volumes were only significantly different in the case of the medium scenario (Figure 7).

643 These differences in the methodologies result in differences in the outcomes, in terms of the
644 **potential and estimated wood supply**. The EGA generally produced larger potential recruitment
645 areas. The volume reduction factors applied in EGA are, however, on average much smaller than
646 the respective fuzzy-logic values created in FGA (Figure S3). As a result, estimated wood supply
647 is generally larger for FGA, as shown in section 4.1. For our test catchments, the application of
648 simple empirical volume reduction factors as part of the EGA model has proven to be similarly
649 accurate in estimating LW volumes, in comparison with a spatially explicit approach such as the
650 FGA model. Still, both the expert-based buffer widths and the reduction factors were defined for
651 the test catchments and validated for similar catchments located in the Alps and pre-Alps, and so
652 they should be carefully tested if applied to other rivers with different characteristics. The fuzzy
653 logic approach indirectly includes this uncertainty or imprecise information (i.e., buffer widths
654 and volume reduction factors), and allows being computed without prior existing observations or

655 knowledge. In both cases, the two models may over- or underestimate the wood volumes, but
656 allow reliable computation of wood supply volumes at the catchment scale and for three scenarios.

657

658 5.2 Qualitative comparison of EGA and FGA with other similar 659 approaches

660 As described in the introduction, only a few approaches have been proposed to compute
661 wood supply at the catchment scale considering different recruitment processes (e.g., landslides,
662 debris flows, bank erosion). Most of the model frameworks described in section 2, particularly
663 those based on GIS and geoprocessing (e.g., Mazzorana et al., 2009), do not attempt to simulate
664 the actual recruitment processes, but use existing information on areas susceptible to certain
665 processes (like the EGA and FGA) from hazard maps or other sources or apply expert-based
666 buffers (like the EGA). Most existing models simulate only one recruitment process explicitly,
667 i.e., landslides or bank erosion (Lucía et al., 2015a; Cislaghi et al., 2018; Zischg et al., 2018;
668 Gasser et al.; 2018, 2020), and a few consider mass movements and fluvial processes (e.g.,
669 Franceschi et al.,2019). Yet, a model that simulates coupled processes to compute wood supply
670 is still lacking. In existing approaches, physically based models are combined with empirical
671 approaches to identify recruitment areas from one single process and compute wood supply at the
672 catchment scale. Still, these models require additional input data, such as precipitation, discharge,
673 soil characteristics etc., which is usually not available or challenging to obtained at the desired
674 resolution. In addition, they are much more expensive in terms of computational time, which
675 limits their application to larger areas. Therefore, there is a gap between the current state-of-the-
676 art of geomorphic process modelling and wood recruitment and supply estimation.

677 Moreover, the majority of existing models used to predict wood supply are deterministic,
678 in that they do not consider the natural process variability and parameter uncertainties. Only the
679 fuzzy logic approach (Ruiz-Villanueva et al., 2014c; Ruiz-Villanueva and Stoffel, 2018)
680 indirectly considers uncertainty, but it does not represent a description of the physical supply
681 processes. A few stochastic models have been proposed (e.g., Bragg, 2000; Eaton et al., 2012;

682 Gregory et al., 2003) to simulate wood recruitment, but they were designed to work at the scale
683 of the river reach only. At the catchment scale, a probabilistic multi-dimensional approach has
684 recently been proposed (Cislaghi et al., 2018) to study wood sources from hillslopes, modelling
685 areas susceptible to landslides, but it neglects other processes such as bank erosion. The latter
686 process has been considered in one of the most recent studies on LW (Gasser et al., 2020).

687 On the other hand, empirical estimation formulas (e.g., Steeb, 2018; Rickenmann, 1997;
688 Uchiogi et al., 1996) are easier and faster to apply to estimate LW supply. However, they provide
689 only an estimate for the whole catchment under investigation, without any spatial differentiation.
690 EGA and FGA, on the other hand, support a comprehensive spatial overview and direct attention
691 to areas in which a more precise assessment of the instream wood situation is necessary, e.g.,
692 through field surveys or expert assessments. Figure S5 shows that the EGA and FGA modelling
693 results approximately correspond to the 50-90% relation between V_{obs} and catchment area as
694 described with the empirical formula of Steeb (2018).

695

696 ### 5.3 Uncertainty in the observed and modelled LW volumes

697 The two GIS approaches presented here yielded similar orders of magnitude of LW supply
698 for a given catchment and for the three designed scenarios. Still, several uncertainties associated
699 with the estimation of LW supply remain, and they are not just related to the obtained results and
700 the applied methodologies, but also to the available observations (coming from surveys after flood
701 events) used for calibration and validation.

702 The observed wood volumes V_{obs} were compiled mostly from technical reports of post-
703 event analyses, and these values might be in some cases only rough estimates, with a considerable
704 uncertainty. LW volumes were estimated based on LW deposits and piles in the field, for which
705 the volume and the corresponding wood content (or pore volume, respectively) must be estimated.
706 The assessment of the wood volume of such accumulations might be challenging and uncertainty
707 might be high (Spreitzer et al., 2020; Thevenet et al., 1998). Some of the observed wood volumes

708 V_{obs} were also determined based on forest loss areas, for which a pre-event forest density value W
709 must be assumed. In the analysis made with the GIS models, the forest density raster map of
710 Ginzler et al. (2019) was used, which may differ from values used during the post event surveys.
711 Furthermore, the time gap between a LW transporting flood event and the survey year on which
712 the forest density map is derived from, needs to be accounted for. Depending on this relationship,
713 wood volumes may be underestimated (i.e., survey year after flood event) or overestimated (i.e.,
714 survey year before flood event). This circumstance could also explain why in some cases of the
715 FGA calculations the potential wood volume is even smaller than the observed wood volume
716 ($V_{obs}/V_{pot} > 1$; see Figure 10a). This discrepancy appeared mostly in one large catchment (i.e.,
717 Chirel) and its subcatchments (i.e., Fildrich, Goldbach, Rütigrabe), and could be related to the
718 forest density data used to compute the wood supply volumes, which was computed with the
719 forest after the large flood in 2005.

720 The observations we used remain a unique and extensive dataset (Steeb et al., 2019a),
721 which allowed us to parametrize the models more accurately. The EGA uses empirical volume
722 reduction factors that were derived from this dataset for the conversion of V_{pot} to V_{est}. In case of
723 debris flows, for example, the volume reduction factors f also rely on an event analysis of the
724 August 2005 flood in Switzerland by Rickenmann et al. (2008), who showed that, on average, 11-
725 19 % of all torrents in the main investigated mountain river catchments were associated with
726 debris flow activity. This percentage range was used to define the reduction factors as shown in
727 Table 2. This highlights the importance of in-depth post flood event analyses, as these provide
728 valuable empirical datasets that can be used to validate and further develop models to estimate
729 supplied LW volumes. The application of models should not replace field work surveys, but they
730 should be used in a complementary manner.

731 Another source of uncertainty is given by the SilvaProtect-CH trajectories. Since their input
732 data, in particular geology, provide a large-scale representation of natural conditions (see text in
733 the supplementary material), the SilvaProtect-CH trajectories are best suitable for use on a
734 catchment-scale range. Furthermore, SilvaProtect-CH trajectories generally result in a pessimistic

picture under unfavourable conditions (e.g., no consideration of the stabilizing influence of vegetation cover). As a consequence, only a small part of the trajectories is expected to be active during rainfall and consequent floods. In addition, the actual run-out zones of mass wasting processes may often be shorter than the modelled trajectories.

One important limitation of the EGA and FGA models presented in this study is that the available input forest cover, does not provide any further information about the forest typology, structure, and species composition. Despite the role that differences in forest may play in stabilizing the soil and slopes and in influencing bank erosion and hillslope stability (Gasser et al., 2019), the two methods do not explicitly consider this effect. Moreover, the type, structure and stage of forest stand control the extent to which trees can be uprooted and recruited and supplied to rivers (Mazzorana et al., 2009; Ruiz-Villanueva et al., 2014c). This aspect was described as the vegetation resistance defined by Ruiz-Villanueva et al. (2014c) based on the tree species and forest stage, the structural classification of forested areas made by Blaschke et al. (2004) and the availability indicator used by Mazzorana et al. (2009). Unlike in the approach used by Franceschi et al. (2019) or Gasser et al. (2018), who detected individual trees from high-resolution LiDAR data, in our case there was no information available with the spatial resolution required to take account for the dimensions, proportion of different species, the stage (e.g., remnant or reforested) or the age of the forest stand. Neglecting the different response of different forest types may result in an overestimation of supplied volumes.

As discussed above, modelling and quantification of wood supply volumes is characterised by many uncertainties. After all, the two models presented in this study allow quantifying the magnitude of the expected LW supply, thus further expert judgement and knowledge of local (geomorphic) characteristics is required to adequately interpret the results. The ratio between predicted and observed LW volumes varies by about 1-2 order of magnitudes. For comparison it is noted that a similar or even larger range of uncertainty can be expected for the estimation of bedload volumes transported during floods (e.g., Rickenmann and Koschni, 2010).

5.4 Implications for hazard assessment and river management

From a practical perspective, geospatial LW modelling results can be used for hazard assessment, infrastructure design, and the definition of management strategies. From a scientific perspective, further applications are possible. For example, estimated wood volumes can be applied as an input for a wood transport model, such as Iber-Wood (Ruiz-Villanueva et al., 2014a, 2014b, 2015) or other approaches (e.g., Mazzorana et al., 2011), to define realistic boundary conditions. Furthermore, if no observation data are available for reference, estimated wood volumes from EGA and FGA can be used to quantify blocking probabilities due to LW at bridge piers or at other critical cross-section (Schalko, 2019; Schalko et al., 2018; Schmocker and Weitbrecht, 2013).

As described in section 4.2, the average proportion of instream deadwood (instream wood load) from the total potential LW supply in the 40 test catchments ranged between 2-13 % (Figure 6). This range is confirmed by other studies and event analyses (Dixon, 2013; Rickli et al., 2018; Waldner et al., 2009). It can be concluded that instream deadwood generally accounted for only a small proportion of the total LW transported during past floods in Switzerland. Rather, it is freshly recruited wood that made up the majority of the transported wood volumes. Deadwood alone, both on the forest floor and in the channel itself, may therefore only lead to a limited increase in risk from a natural hazard management perspective. As a consequence, the artificial removal of deadwood from the stream and its surroundings is not always necessary, keeping in mind the ecological benefits of instream wood.

EGA and FGA are area-wide products that can be applied in any Swiss catchment. They use a standardized procedure and nationwide homogeneous data, which facilitates a comparison between catchments (FOEN, 2019). The methodology is flexible and can be adapted to other regions outside Switzerland if recruitment processes (especially with regard to SilvaProtect-CH trajectories) were modelled with more generic approaches.

Both models have already been used by practitioners for some engineering applications. One limitation that has been identified by some practitioners is the use of licensed software, as

789 both EGA and FGA have been developed in ESRI software and require some advanced licenses
790 that may not always be available to private companies. Future developments may consider the
791 migration to open-source software.

792 Furthermore, there is still a need to analyse and model the propagation of LW through the
793 river network, for example by applying hydraulic modelling (e.g., Ruiz-Villanueva et al., 2014)
794 or the recently proposed network approaches such as those applied to sediment transfer (Finch
795 and Ruiz-Villanueva, 2022).

796 The two models presented here correspond to a hazard index mapping in terms of
797 processing depth and degree of detail for a hazard assessment. The geospatial modelling results
798 indicate areas of potential LW recruitment, however without precise information on the intensities
799 occurring or the transfer and propagation through the river network. In contrast, the estimated LW
800 supply for the large scenario is based on the data of events with a return period of approximately
801 50 to 150 years. The approach presented here is a useful tool to give a comprehensive overview
802 and direct attention to areas where a more precise assessment of the LW situation is probably
803 useful, for example in connection with an estimation of sediment loads in torrents.

804

805 # 6 CONCLUSIONS

806 Two GIS-based models are presented in this contribution to identify large wood (LW)
807 sources and to estimate LW supply to rivers. Both models, called empirical GIS approach (EGA)
808 and Fuzzy-Logic GIS approach (FGA), consider landslides, debris flows, bank erosion, and
809 mobilization of instream wood as recruitment processes. The results are volumetric estimates of
810 LW supply based on three different scenarios of process frequency and magnitude. Results of
811 model applications to 40 Swiss catchments were used to compare both the two models with each
812 other and the performance in relation to observed (empirical) LW volumes. Further, a literature
813 review of existing LW supply models proposed in the last 35 years was conducted, set into context
814 and remaining challenges were identified.

EGA shows significantly higher values for potential LW supply. However, after reducing the potential volume with different methods, estimated LW supply volumes are in the same order of magnitude for both models, with FGA showing generally somewhat larger values. In case of EGA, landslides are the dominant recruitment process, whereas bank erosion is dominant for FGA. Both models show under- and overestimation of observed wood volumes V_{obs}, with more tendency for overestimation. Overestimation stays generally within two orders of magnitude (typically larger values for FGA), underestimation within on order of magnitude (typically smaller values for EGA).

The modelling and quantification of wood supply volumes is characterised by many uncertainties. After all, the two models presented in this study allow quantifying the magnitude of the expected LW supply, thus further expert judgement and knowledge of local (geomorphic) characteristics is required to adequately interpret such results. LW supply modelling can be further improved by integrating more physically-based and/or probabilistic inputs for the spatial identification of recruitment processes. Likewise, the parametrization and validation of LW supply models remain complex. Post flood event analysis provide valuable empirical datasets that can be used to validate results and further develop LW supply models that can be useful for hazard assessment, infrastructure design, and the definition of management strategies.

ACKNOWLEDGEMENTS

We thank the Swiss Federal Office for the Environment (FOEN) for funding the research program "Large Wood Management in Rivers" (WoodFlow research program; contract no. 15.0018.PJ/O192-3154).

Special thanks go to Peter Waldner (WSL) for providing valuable empirical data from flood events; Benjamin Kuratli (formerly University of Zurich) for helping to develop earlier versions of the EGA; Bronwyn Price, Christian Ginzler and Markus Huber (all WSL) for providing data from the Swiss National Forest Inventory; and finally, Stéphane Losey (FOEN) for providing all the required SilvaProtect-CH data.

REFERENCES

Bachmann Walker, A. 2012. Ausmass und Auftreten von Seitenerosionen bei Hochwasser. Auswertung von hydraulisch verursachten Seitenerosionen und Herleitung von empirischen Zusammenhängen zur Ermittlung des Erosionsausmasses und -auftreten. Master thesis. Geographisches Institut der Universität Bern (in German).

Beechie TJ, Pess G, Kennard P, Bilby RE, Bolton S. 2000. Modeling Recovery Rates and Pathways for Woody Debris Recruitment in Northwestern Washington Streams. North American Journal of Fisheries Management 20 : 436–452. DOI: 10.1577/1548-8675(2000)020<0436:mrrapf>2.3.co;2

Benda LE, Litschert SE, Reeves G, Pabst R. 2016. Thinning and in-stream wood recruitment in riparian second growth forests in coastal Oregon and the use of buffers and tree tipping as mitigation. Journal of Forestry Research 27 : 821–836. DOI: 10.1007/s11676-015-0173-2

Benda L, Bigelow P. 2014. On the patterns and processes of wood in northern California streams. Geomorphology 209 : 79–97. DOI: 10.1016/j.geomorph.2013.11.028

Benda L, Miller D, Andras K, Bigelow P, Reeves G, Michael D. 2007. NetMap: A new tool in support of watershed science and resource management. Forest Science 53 : 206–219. DOI: 10.1093/forestscience/53.2.206

Benda LE, Sias JC. 2003. A quantitative framework for evaluating the mass balance of in-stream organic debris. Forest Ecology and Management 172 : 1–16. DOI: 10.1016/S0378-1127(01)00576-X

Bezzola GR, Gantenbein S, Hollenstein R, Minor HE. 2002. Verklausung von Brückenquerschnitten; Internationales Symposium Moderne Methoden und Konzepte im Wasserbau; Mitteilung der Versuchsanstalt für Wasserbau, Hydrologie und Glaziologie der ETH Zürich, Nr. 175

Bishop MP, Giardino JR 2022. Chapter 1.01 - Technology-Driven Geomorphology: Introduction and Overview. In: Editor(s): John (Jack) F. Shroder, Treatise on Geomorphology (Second Edition), Academic Press, 2022, Pages 1-17. ISBN 9780128182352, DOI: 10.1016/B978-0-12-818234-5.00171-1.

Blaschke T, Tiede D, Heurich M. 2004. 3D landscape metrics to modelling forest structure and diversity based on laser scanning data. International Archives of the Photogrammetry, Remote Sensing and Spatial Information Sciences XXXVI-8W2 : 129–132.

Bonham-Carter GF, Agterberg FP, Wright DF. 1990. Weights of evidence modelling: a new approach to mapping mineral potential. In Statistical applications in the earth sciences,

875 Paper89-9 , Agterberg FP and Bonham-Carter G (eds). Canadian Government Publishing
876 Centre: Ottawa, Ontario, Canada; 171–183.

877 Bragg DC. 2000. Simulating catastrophic and individualistic large woody debris recruitment for
878 a small riparian system. Ecology 81 : 1383. DOI: 10.2307/177215

879 Braudrick CA, Grant GE, Ishikawa Y, Ikeda H. 1997. Dynamics of wood transport in streams: A
880 flume experiment. Earth Surface Processes and Landforms 22 : 669–683. DOI:
881 10.1002/(SICI)1096-9837(199707)22:7<669::AID-ESP740>3.3.CO;2-C

882 Cavalli M, Trevisani S, Comiti F, Marchi L. 2013. Geomorphometric assessment of spatial
883 sediment connectivity in small Alpine catchments. Geomorphology 188 : 31–41. DOI:
884 10.1016/j.geomorph.2012.05.007

885 Cislaghi A, Rigon E, Lenzi MA, Bischetti GB. 2018. A probabilistic multidimensional approach
886 to quantify large wood recruitment from hillslopes in mountainous-forested catchments.
887 Geomorphology 306 : 108–127. DOI: 10.1016/j.geomorph.2018.01.009

888 Comiti F, Lucía A, Rickenmann D. 2016. Large wood recruitment and transport during large
889 floods: A review. Geomorphology 269: 23–39. DOI: 10.1016/j.geomorph.2016.06.016

890 Dixon SJ. 2013. Investigating the effects of large wood and forest management on flood risk and
891 flood hydrology, University of Southhampton

892 Dorren L. 2017. FINT – Find individual trees. User manual. ecorisQ paper.

893 Downs PW, Simon A. 2001. Fluvial geomorphological analysis of the recruitment of large woody
894 debris in the Yalobusha river network, Central Mississippi, USA. Geomorphology 37 : 65–91.
895 DOI: 10.1016/S0169-555X(00)00063-5

896 Eaton BC, Hassan MA, Davidson SL. 2012. Modeling wood dynamics, jam formation, and
897 sediment storage in a gravel-bed stream. Journal of Geophysical Research: Earth Surface 117:
898 1–18. DOI: 10.1029/2012JF002385

899 Finch B, Ruiz-Villanueva V. 2022. Exploring the potential of the Graph Theory to large wood
900 supply and transfer in river networks. EGU22-8232. DOI: 10.5194/egusphere-egu22-8232
901 EGU General Assembly 2022.

902 FOEN. 2019. Schwemmholz in Fliessgewässern. Ein praxisorientiertes Forschungsprojekt.
903 Bundesamt für Umwelt, Bern. Umwelt-Wissen Nr. 1910, 100 p.

904 FOEN. 2015. Einzugsgebietsgliederung Schweiz, EZGG-CH. Bundesamt für Umwelt, Bern.
905 http://www.bafu.admin.ch/ezgg-ch

Franceschi S, Antonello A, Vela AL, Cavalli M, Crema S, Tonon G, Comiti F. 2019. GIS-based approach to assess large wood transport in mountain rivers during floods. Preprint DOI: 10.13140/RG.2.2.31787.08480

Gasser E, Perona P, Dorren L, Phillips C, Hübl J, Schwarz M. 2020. A new framework to model hydraulic bank erosion considering the effects of roots. Water (Switzerland) 12 DOI: 10.3390/w12030893

Gasser E, Schwarz M, Simon A, Perona P, Phillips C, Hübl J, Dorren L. 2019. A review of modeling the effects of vegetation on large wood recruitment processes in mountain catchments. Earth-Science Reviews 194 : 350–373. DOI: 10.1016/j.earscirev.2019.04.013

Gasser E, Simon A, Perona P, Dorren L, Hübl J, Schwarz M. 2018. Quantification of potential recruitment of large woody debris in mountain catchments considering the effects of vegetation on hydraulic and geotechnical bank erosion and shallow landslides. Paquier A and Rivière N (eds). E3S Web of Conferences 40 DOI: 10.1051/e3sconf/20184002046

Ginzler C, Price B, Bösch R, Fischer C, Hobi ML, Psomas A, Rehush N, Wang Z, Waser LT. 2019. Area-Wide Products. In Swiss National Forest Inventory – Methods and Models of the Fourth Assessment , Fischer C and Traub B (eds). Springer International Publishing: Cham; 125–142.

von Glutz M. 2011. Verfahren zur Abschätzung des Schwemmholzpotentials von Wildbächen. Bachelor thesis. Schweizerische Hochschule für Landwirtschaft (SHL), Zollikofen, Switzerland. 116 p. (in German)

Gregory SV, Meleason MA, Sobota DJ. 2003. Modeling the dynamics of wood in streams and rivers. In American Fisheries Society Symposium 37 , Gregory S V., Boyer K, and Gurnell A (eds). 315–335.

Gurnell AM, Bertoldi W. 2020. Wood in Fluvial Systems. 2nd ed. Elsevier Inc. Editor(s): John (Jack) F. Shroder, Treatise on Geomorphology (Second Edition), Academic Press, 2022, Pages 320-352, ISBN 9780128182352. DOI: 10.1016/B978-0-12-409548-9.12415-7

Harmon ME, Franklin JF, Swanson FJ, Sollins P, Gregory SV, Lattin JD, Anderson NH, Cline SP, Aumen NG, Sedell JR, Lienkaemper GW, Cromack K, Cummins KW. 1986. Ecology of coarse woody debris in temperate ecosystems. In: MacFadyen, A.; Ford, E. D., eds. Advances in ecological research. Orlando, FL: Academic Press, Inc.: 15: 133-302.

Hassan MA, Bird S, Reid D, Hogan D. 2016. Simulated wood budgets in two mountain streams. Geomorphology 259 : 119–133. DOI: 10.1016/j.geomorph.2016.02.010

Hunziker G. 2017. Schwemmholz Zulg. Untersuchungen zum Schwemmholzaufkommen in der

939 Zulg und deren Seitenbächen. Hunziker Gefahrenmanagement Bericht (Gemeinde
940 Steffisburg).

941 Hunzinger L, Durrer S. 2008. Seitenerosion, in: Bezzola, G.R., Hegg, C. (Eds.), Ereignisanalyse
942 Hochwasser 2005, Teil 2 – Analyse von Prozessen, Massnahmen Und Gefahrengrundlagen.
943 Umwelt-Wissen, Nr. 0825, Bundesamt für Umwelt BAFU & Eidg. Forschungsanstalt WSL,
944 Bern, pp. 125-136 (in German).

945 Hupp CR, Simon A. 1991. Bank accretion and development of vegetated depositional surfaces
946 along modified alluvial channels, Geomorphology, 4, 111-124.

947 Kasprak A, Magilligan FJ, Nislow KH, Snyder NP. 2012. A LIDAR-derived evaluation of
948 watershed-scale large woody debris sources and recruitment mechanisms: Coastal Maine,
949 USA. River Research and Applications 28 : 1462–1476. DOI: 10.1002/rra.1532

950 Kennard P, Pess G, Beechie T, Bilby R, Berg D. 1999. Riparian-in-a-box: A manager's tool to
951 predict the impacts of riparian management on fish habitat. In Forest–Fish Conference: Land
952 Management Practices Affecting Aquatic Ecosystems. Natural Resources Canada, Canadian
953 Forest Service Information Report NOR-X-356. , Brewin M and Monit D (eds). Calgary,
954 Alberta, Cananda; 483–490.

955 Lassettre NS, Kondolf GM. 2012. Large woody debris in urban stream channels: Redefining the
956 problem. River Research and Applications 28 : 1477–1487. DOI: 10.1002/rra.1538

957 Losey S, Wehrli A. 2013. Schutzwald in der Schweiz. Vom Projekt SilvaProtect-CH zum
958 harmonisierten Schutzwald . Bern, Schweiz

959 Lucía A, Andrea A, Daniela C, Marco C, Stefano C, Silvia F, Enrico M, Martin N, Stefan S,
960 Francesco C. 2015a. Monitoring and Modeling Large Wood Recruitment and Transport in a
961 Mountain Basin of North-Eastern Italy. In Engineering Geology for Society and Territory -
962 Volume 3. Springer International Publishing: Cham; 155–158.

963 Lucía A, Comiti F, Borga M, Cavalli M, Marchi L. 2015b. Dynamics of large wood during a flash
964 flood in two mountain catchments. Natural Hazards and Earth System Sciences 15 : 1741–
965 1755. DOI: 10.5194/nhess-15-1741-2015

966 Lucía A, Schwientek M, Eberle J, Zarfl C. 2018. Planform changes and large wood dynamics in
967 two torrents during a severe flash flood in Braunsbach, Germany 2016. Science of the Total
968 Environment 640–641 : 315–326. DOI: 10.1016/j.scitotenv.2018.05.186

969 Malanson GP, Kupfer JA. 1993. Simulated fate of leaf litter and large woody debris at a riparian
970 cutbank. Canadian Journal of Forest Research 23 : 582–590.

971 Martin D, Benda L. 2001. Patterns of in-stream wood recruitment and transport at the watershed
972 scale. In Transactions of the American Fisheries Society 130 , . 940–958.

973 Mazzorana B, Ruiz-Villanueva V, Marchi L, Cavalli M, Gems B, Gschnitzer T, Mao L, Iroumé
974 A, Valdebenito G. 2018. Assessing and mitigating large wood-related hazards in mountain
975 streams: recent approaches. Journal of Flood Risk Management 11 : 207–222. DOI:
976 10.1111/jfr3.12316

977 Mazzorana B, Hübl J, Zischg A, Largiader A. 2011. Modelling woody material transport and
978 deposition in alpine rivers. Natural Hazards 56 : 425–449. DOI: 10.1007/s11069-009-9492-y

979 Mazzorana B, Zischg A, Largiader A, Hübl J. 2009. Hazard index maps for woody material
980 recruitment and transport in alpine catchments. Natural Hazards and Earth System Science 9 :
981 197–209. DOI: 10.5194/nhess-9-197-2009

982 Meleason MA, Gregory S V., Bolte JP. 2003. Implications of riparian management strategies on
983 wood in streams of the Pacific northwest. Ecological Applications 13 : 1212–1221. DOI:
984 10.1890/02-5004

985 Montgomery DR, Dietrich WE. 1994. A physically based model for the topographic control on
986 shallow landsliding. Water Resources Research 30 : 1153–1171. DOI: 10.1029/93WR02979

987 Montgomery DR, Piégay H. 2003. Wood in rivers: interactions with channel morphology and
988 processes. Geomorphology 51 : 1–5. DOI: 10.1016/S0169-555X(02)00322-7

989 Murphy ML, Koski K V. 1989. Input and Depletion of Woody Debris in Alaska Streams and
990 Implications for Streamside Management. North American Journal of Fisheries Management
991 9 : 427–436. DOI: 10.1577/1548-8675(1989)009<0427:iadowd>2.3.co;2

992 Nakamura F, Seo J Il, Akasaka T, Swanson FJ. 2017. Large wood, sediment, and flow regimes:
993 Their interactions and temporal changes caused by human impacts in Japan. Geomorphology
994 279: 176–187. DOI: 10.1016/j.geomorph.2016.09.001.

995 Piégay H, Thévenet A, Citterio A. 1999. Input, storage and distribution of large woody debris
996 along a mountain river continuum, the Drôme River, France. CATENA 35 : 19–39. DOI:
997 10.1016/S0341-8162(98)00120-9

998 R Core Team. 2019. R: A Language and Environment for Statistical Computing. R Foundation
999 for Statistical Computing, Vienna, Austria. https://www.R-project.org/

1000 Rainville RC, Rainville SC, Linder EL. 1986. Riparian silvicultural strategiesfor fish habitat
1001 emphasis. 186–196 pp.

1002 Rickenmann D. 1997. Schwemmholz und Hochwasser. Wasser, Energie, Luft 89 : 115-119 (in

German).

Rickenmann, D., Canuto, N., Koschni, A. 2008. Ereignisanalyse Hochwasser 2005. Teilprojekt Vertiefung Wildbäche: Einfluss von Lithologie/Geotechnik und Niederschlag auf die Wildbachaktivität beim Hochwasser 2005. Birmensdorf, Switzerland.

Rickenmann, D., Koschni, A. 2010. Sediment loads due to fluvial transport and debris flows during the 2005 flood events in Switzerland. Hydrol. Process. 24, 993–1007. doi:10.1002/hyp.7536

Rickenmann D, Badoux A, Hunzinger L. 2016. Significance of sediment transport processes during piedmont floods: the 2005 flood events in Switzerland. Earth Surface Processes and Landforms 41 : 224–230. DOI: 10.1002/esp.3835

Rickli C, Badoux A, Rickenmann D, Steeb N, Waldner P. 2018. Large wood potential, piece characteristics, and flood effects in Swiss mountain streams. Physical Geography 3646 : 1–23. DOI: 10.1080/02723646.2018.1456310

Rickli, C., McArdell, B., Badoux, A., Loup, B., 2016. Database shallow landslides and hillslope debris flows, in: Koboltschnig, G. (Ed.), 13th Congress INTERPRAEVENT 2016. 30 May to 2 June 2016. Lucerne, Switzerland. International Research Society INTERPRAEVENT, Klagenfurt, Austria, pp. 242–243.

Rickli C, Bucher H. 2006. Einfluss ufernaher Bestockungen auf das Schwemmholzvorkommen in Wildbächen . Eidg. Forschungsanstalt für Wald Schnee und Landschaft WSL: Birmensdorf, 94 pp. (in German)

Rigon E, Comiti F, Lenzi MA. 2012. Large wood storage in streams of the Eastern Italian Alps and the relevance of hillslope processes. Water Resources Research 48 : 1–18. DOI: 10.1029/2010WR009854

Rimböck A. 2001. Luftbildbasierte Abschätzung des Schwemmholzpotentials (LASP) in Wildbächen. In: Festschrift aus Anlass des 75-jährigen Bestehens der Versuchsanstalt für Wasserbau und Wasserwirtschaft der Technischen Universität München in Obernach

Rimböck A. 2003. Schwemmholzrückhalt in Wildbächen: Grundlagen zu Planung und Berechnung von Seilnetzsperren . Ausgabe 94. Lehrstuhl und Versuchsanstalt für Wasserbau und Wasserwirtschaft der Technischen Universität München

Ruiz-Villanueva V, Mazzorana B, Bladé E, Bürkli L, Iribarren-Anacona P, Mao L, Nakamura F, Ravazzolo D, Rickenmann D, Sanz-Ramos M, Stoffel M, Wohl E. 2019. Characterization of wood-laden flows in rivers. Earth Surface Processes and Landforms. https://doi.org/https://doi.org/10.1002/esp.4603

1036 Ruiz-Villanueva V, Bladé Castellet E, Díez-Herrero A, Bodoque JM, Sánchez-Juny M. 2014a.
1037 Two-dimensional modelling of large wood transport during flash floods. Earth Surface
1038 Processes and Landforms 39 : 438–449. DOI: 10.1002/esp.3456

1039 Ruiz-Villanueva V, Bladé E, Sánchez-Juny M, Marti-Cardona B, Díez-Herrero A, Bodoque JM.
1040 2014b. Two-dimensional numerical modeling of wood transport. Journal of Hydroinformatics
1041 16 : 1077. DOI: 10.2166/hydro.2014.026

1042 Ruiz-Villanueva V, Díez-Herrero A, Ballesteros JA, Bodoque JM. 2014c. Potential large woody
1043 debris recruitment due to landslides, bank erosion and floods in mountain basins: a quantitative
1044 estimation approach. River Research and Applications 30 : 81–97. DOI: 10.1002/rra.2614

1045 Ruiz-Villanueva V, Piégay H, Gurnell AM, Marston RA, Stoffel M. 2016. Recent advances
1046 quantifying the large wood dynamics in river basins: New methods and remaining challenges.
1047 Reviews of Geophysics 54 : 611–652. DOI: 10.1002/2015RG000514

1048 Ruiz-Villanueva V, Stoffel M. 2018. Application of fuzzy logic to large organic matter
1049 recruitment in forested river basins. Proceedings ofthe 5th IAHREurope Congress —New
1050 Challenges in Hydraulic Research and Engineering : 467–468. DOI: 10.3850/978-981-11-
1051 2731-1_047-cd

1052 Ruiz-Villanueva V, Wyzga B, Zawiejska J, Hajdukiewicz M, Stoffel M. 2015. Factors controlling
1053 large-wood transport in a mountain river. Geomorphology DOI:
1054 10.1016/j.geomorph.2015.04.004

1055 Ruiz-Villanueva V, Bodoque JM, Díez-Herrero A, Eguibar MA, Pardo-Igúzquiza E. 2013.
1056 Reconstruction of a flash flood with large wood transport and its influence on hazard patterns
1057 in an ungauged mountain basin. Hydrological Processes 27 : 3424–3437. DOI:
1058 10.1002/hyp.9433

1059 Ruiz-Villanueva V, Gamberini C, Bladé E, Stoffel M, Bertoldi W. 2020. Numerical Modeling of
1060 Instream Wood Transport, Deposition, and Accumulation in Braided Morphologies Under
1061 Unsteady Conditions: Sensitivity and High-Resolution Quantitative Model Validation. Water
1062 Resources Research 56 : 1–22. DOI: 10.1029/2019WR026221

1063 Ruiz-Villanueva V, Badoux A, Rickenmann D, Böckli M, Schläfli S, Steeb N, Stoffel M, Rickli
1064 C. 2018. Impacts of a large flood along a mountain river basin: the importance of channel
1065 widening and estimating the large wood budget in the upper Emme River (Switzerland). Earth
1066 Surface Dynamics, June, 1–42. https://doi.org/https://doi.org/10.5194/esurf-6-1115-2018

1067 RStudio Team. 2021. RStudio: Integrated Development Environment for R. RStudio, PBC,
1068 Boston, MA URL http://www.rstudio.com/

Simon A. 1989. Shear-strength determination and stream-bank instabil- ity in loess-derived alluvium, West Tennessee, USA, in Applied Quaternary Research, edited by E. J. DeMulder and B. P. Hageman, pp. 129-146, A. A. Balkema Publications, Rotterdam.

Schalko I. 2019. Laboratory Flume Experiments on the Formation of Spanwise Large Wood Accumulations : I. Effect on Backwater Rise Water Resources Research. DOI: 10.1029/2018WR024649

Schalko I, Schmocker L, Weitbrecht V, Boes RM. 2018. Backwater Rise due to Large Wood Accumulations. Journal of Hydraulic Engineering 144 : 04018056. DOI: 10.1061/(ASCE)HY.1943-7900.0001501

Schloerke B, Cook D, Larmarange J, Briatte F, Marbach M, Thoen E, Elberg A, Crowley J. 2021. GGally: Extension to 'ggplot2'. R package version 2.1.2. https://CRAN.R-project.org/package=GGally

Schmocker L, Weitbrecht V. 2013. Driftwood : Risk Analysis and Engineering Measures. Journal of Hydraulic Engineering 139 : 683–695. DOI: 10.1061/(ASCE)HY.1943-7900.0000728.

Seo J, Nakamura F, Chun KW. 2010. Dynamics of large wood at the watershed scale: A perspective on current research limits and future directions. Landscape and Ecological Engineering 6 : 271–287. DOI: 10.1007/s11355-010-0106-3

Van Sickle J, Gregory S V. 1990. Modeling inputs of large woody debris to streams from falling trees. Canadian Journal of Forest Research 20 : 1593–1601. DOI: 10.1139/x90-211

Spreitzer G, Tunnicliffe J, Friedrich H. 2020. Porosity and volume assessments of large wood (LW) accumulations. Geomorphology 358 : 107122. DOI: 10.1016/j.geomorph.2020.107122

Steeb N, Badoux A, Rickli C, Rickenmann D. 2022. Empirical prediction of large wood transport during flood events. 11th IHAR International Conference on Fluvial Hydraulics, River Flow 2022. Kingston and Ottawa, November 8-10, 2022.

Steeb N, Rickenmann D, Rickli C, Badoux A. 2021. Large wood event database. EnviDat. https://www.envidat.ch/dataset/large-wood-event-database

Steeb N, Badoux A, Rickli C, Rickenmann D. 2019a. Detailbericht zum Forschungsprojekt WoodFlow: Empirische Schätzformeln. Birmensdorf

Steeb N, Badoux A, Rickli C, Rickenmann D. 2019b. Detailbericht zum Forschungsprojekt WoodFlow: Empirischer GIS-Ansatz. Birmensdorf

Steeb N. 2018. Empirical prediction of large wood transport during flood events. 5th IHAR Europe Congress. New challenges in Hydraulic Research and Engineering. Trento, Italy.

Steeb N, Kuratli B, Rickli C, Badoux A, Rickenmann D. 2017a. GIS-Modellierung des Schwemmholzpotentials in alpinen Einzugsgebieten. Agenda FAN 2/2017 2 : 9–12.

Steeb N, Rickenmann D, Badoux A, Rickli C, Waldner P. 2017b. Large wood recruitment processes and transported volumes in Swiss mountain streams during the extreme flood of August 2005. Geomorphology 279 : 112–127. DOI: https://doi.org/10.1016/j.geomorph.2016.10.011

Steel EA, Richards WH, Kelsley KA. 2003. Wood and wildlife: Benefits of river wood to terrestrial and aquatic vertebrates. In The ecology and Management of Wood in World Rivers. American Fisheries Society Symposium 37 , Gregory S, Boyer K, and Gurnell A (eds). 235–247.

Strahler AN. 1957. Quantitative analysis of watershed geomorphology. Eos, Transactions American Geophysical Union 38 : 913–920. DOI: 10.1029/TR038i006p00913

Thevenet A, Citterio A, Piegay H. 1998. A new methodology for the assessment of large woody debris accumulations on highly modified rivers (example of two French Piedmont rivers). Regulated Rivers: Research & Management 14 : 467–483. DOI: 10.1002/(SICI)1099-1646(1998110)14:6<467::AID-RRR514>3.0.CO;2-X

Uchiogi T, Shima J, Tajima H, Ishikawa Y. 1996. Design Methods for Wood-Debris Entrapment. 279–288 pp.

Waldner P et al. 2009. Schwemmholz des Hochwassers 2005. Schlussbericht des WSL-Teilprojekts Schwemmholz der Ereignisanalyse BAFU/WSL des Hochwassers 2005. . Birmensdorf, 70 pp. (in German)

Welty JJ, Beechie T, Sullivan K, Hyink DM, Bilby RE, Andrus C, Pess G. 2002. Riparian aquatic interaction simulator (RAIS): A model of riparian forest dynamics for the generation of large woody debris and shade. Forest Ecology and Management 162: 299–318. DOI: 10.1016/S0378-1127(01)00524-2

Wohl E, Kramer N, Ruiz-Villanueva V, Scott DN, Comiti F, Gurnell AM, Piegay H, Lininger KB, Jaeger KL, Walters DM, Fausch KD. 2019. The Natural Wood Regime in Rivers. BioScience 69 (4), 259–273. DOI: 10.1093/biosci/biz013

Wohl E, Scott DN. 2016. Wood and sediment storage and dynamics in river corridors. Earth Surface Processes and Landforms 42, 5-23. DOI: 10.1002/esp.3909

Wohl E. 2017. Bridging the gaps: An overview of wood across time and space in diverse rivers. Geomorphology, 279, 3–26. https://doi.org/10.1016/j.geomorph.2016.04.014

1133 Wondzell SM, Bisson PA. 2003. Influence of wood on aquatic biodiversity. In The ecology and
1134 Management of Wood in World Rivers. American Fisheries Society Symposium 37 , Gregory
1135 S, Boyer K, and Gurnell A (eds). Bethesda, Maryland; 249–263.

1136 WSL. 2016. Schweizerisches Landesforstinventar LFI. Daten der Erhebungen 2004/06 (LFI3)
1137 und 2009/13 (LFI4). Markus Huber 06.06.2016.

1138 Zeh Weissmann H, Könitzer C, Bertiller A. 2009. Strukturen der Fliessgewässer in der Schweiz.
1139 Zustand von Sohle, Ufer und Umland (Ökomorphologie); Ergebnisse der
1140 ökomorphologischen Kartierung. Umwelt-Zustand Nr. 0926 . Bern

1141 Zischg AP, Galatioto N, Deplazes S, Weingartner R, Mazzorana B. 2018. Modelling
1142 spatiotemporal dynamics of large wood recruitment, transport, and deposition at the river reach
1143 scale during extreme floods. Water (Switzerland) 10 : 1134. DOI: 10.3390/w10091134